JOURNAL OF ENGINEERING RESEARCH & SCIENCES

JENRS

www.jenrs.com
ISSN: 2831-4085

Volume 1 Issue 11
November 2022

EDITORIAL BOARD

Editor-in-Chief

Editorial Board Members

Editorial

This collection of these three research papers presents pioneering advancements across various domains, from enhancing our understanding of occupant behaviour in built environments to developing cost-effective health monitoring devices and improving the performance of recycled asphalt materials. Each study exemplifies the importance of integrating diverse methodologies and perspectives to address contemporary challenges.

The first paper highlights a novel approach to studying occupant behaviour by incorporating psychological, physiological, social, and temporal factors, alongside traditional environmental and contextual elements. Using Interaction Geography in a Virtual Reality (VR) museum, the study reveals how personal connections and study majors influence participants' exploration and time spent in the VR space. This comprehensive approach opens new avenues for understanding human interactions within built environments, offering valuable insights for designing more responsive and engaging spaces [1].

In the realm of cardiovascular health, the second paper addresses the critical need for accessible and accurate diagnostic tools in developing countries. By creating a low-cost, portable ECG device integrated with HealthyPi v3, a raspberry pi-based vital sign monitor, the researchers provide a sustainable solution for early detection and monitoring of cardiovascular diseases. The device captures real-time ECG data and other vital signs, employing advanced machine learning algorithms such as Support Vector Machine (SVM), Convolutional Neural Network (CNN), and Recurrent Neural Network (RNN) for accurate heart disease prediction. This innovation promises to enhance healthcare delivery and outcomes in resource-limited settings [2].

The third paper delves into the use of recycled asphalt shingles (RAS) in asphalt mixtures, addressing the challenges posed by the aged and oxidized RAS binder. The researchers introduce an innovative technique involving the interaction of RAS particles with rejuvenators before mixing with the asphalt binder. This approach compensates for the loss of low-molecular-weight fractions in the RAS, improving the modified binders' fatigue and thermal cracking resistance. By utilizing various rejuvenators, including pyrolysis oils and recycling agents, the study demonstrates how different particle sizes and rejuvenator types affect the stiffness and elasticity of the asphalt binders. These findings pave the way for more durable and sustainable asphalt materials, contributing to the broader goal of environmental conservation [3].

Collectively, these papers showcase the transformative potential of interdisciplinary research in solving complex problems and advancing knowledge across diverse fields. From enhancing occupant experience and healthcare accessibility to improving infrastructure sustainability, these studies highlight the critical role of innovation in shaping a better future.

References:

[1] H. Vo, P. Huesemann-Odom, “Using Interaction Geography to Explore Building Occupant Behaviors in Virtual Reality: A Pilot Study,” *Journal of Engineering Research and Sciences*, vol. 1, no. 11, pp. 1–7, 2022, doi:10.55708/js0111001.

[2] S.Md.R. Islam, A. Hossain, A. Abdullah, “Real-Time Acquisition and Classification of Electrocardiogram Signal,” *Journal of Engineering Research and Sciences*, vol. 1, no. 11, pp. 8–15, 2022, doi:10.55708/js0111002.

[3] E. Deef-Allah, M. Abdelrahman, “Enhancing the Contribution of Recycled Asphalt Shingles to Asphalt Binders Using Rejuvenators,” *Journal of Engineering Research and Sciences*, vol. 1, no. 11, pp. 16–33, 2022, doi:10.55708/js0111003.

Editor-in-chief

Prof. Paul Andrew

JOURNAL OF ENGINEERING RESEARCH AND SCIENCES

Volume 1 Issue 11 November 2022

CONTENTS

Using Interaction Geography to Explore Building Occupant Behaviors in Virtual Reality: A Pilot Study 01
Hoa Vo, Peter Huesemann-Odom

Real-Time Acquisition and Classification of Electrocardiogram Signal 08
Sheikh Md. Rabiul Islam, Akram Hossain, Asif Abdullah

Enhancing the Contribution of Recycled Asphalt Shingles to Asphalt Binders Using Rejuvenators 16
Eslam Deef-Allah, Magdy Abdelrahman

Received: 08 September 2022, Revised: 11 November 2022, Accepted: 12 November 2022, Online: 27 November 2022

DOI: https://dx.doi.org/10.55708/js0111001

Using Interaction Geography to Explore Building Occupant Behaviors in Virtual Reality: A Pilot Study

Hoa Vo*, Peter Huesemann-Odom

Welch School of Art and Design, College of the Arts, Georgia State University, Atlanta, 30303, USA
*Corresponding author: Hoa Vo, AH 362,10 Peachtree Center Ave. SE, Atlanta, GA 30303, USA, (+1)404-413-5143, kvo@gsu.edu

ABSTRACT: The sole focus of current occupant behavior research on environmental and contextual factors (i.e., physical attributes) in buildings is a missed opportunity. Psychological, physiological, social, time, and random factors also influence building occupants. In this pilot study ($n = 10$), the authors used Interaction Geography to capture human movements across space and time in a Virtual Reality (VR) museum to dissect building occupant behavior. Results indicated that study majors (i.e., psychological) and personal connections (i.e., social) with the space affected how participants explored and spent time in the VR museum.

KEYWORDS: Interaction Geography, Building Occupant Behavior, Virtual Reality

1. Introduction

Building occupant behaviors are the direct indicators of how well the built environment (e.g., interior spaces) promotes human physical and psychological well-being. The current approach to comprehending said behaviors focuses on occupant assessments of the physical design or subjective ratings of indoor environmental quality (IEQ) factors such as acoustics, cleanliness, and furnishings [1]. Occupancy evaluations exemplify this approach by asking occupants to rate their satisfaction with IEQ factors on survey-based Likert-scale items (e.g., 1 = dissatisfied; 7 = satisfied) [2]. This approach may seem like an objective way to measure IEQ; however, the following problems cloud the resulting data. First, retrospective data collection relies on occupants' memories of a space. Subjects might mis-remember or fail to recall their experience with the building [3]. Therefore, their ratings of IEQ factors are inadequate and incomplete reflections of their real-time experiences which dictate their behaviors in the building. Second, the tendency to reduce cognitive load means that occupants frequently select the middle choice of complex multiple-choice questions [4].

These biases challenge researchers who study the built environment to develop more comprehensive methods for assessing occupants' behaviors. One exemplary method is implementing agent-based simulation (ABS), autonomous computational agents interacting with one another and their surroundings [5], to predict occupant behaviors in buildings. ABS is most effective in modeling behavioral patterns in hypothesized scenarios to schedule working shifts, regulate energy usage, evacuate for emergencies, and so on [6–8]. One caveat of using ABS in the built environment is that the computational system disregards the complexities underlying occupant behaviors (e.g., age, gender, and psychological state) [6]. This argument also applies to sensor-based and GPS-enabled data collection, with a heavy emphasis on the physical characteristics of the building, not the psychological aspects of occupants [9], [10].

Interaction geography, a novel approach to describing, representing, and interpreting human interactions with their environments across space and time [11], offers one solution to these challenges. Current implementations of interaction geography in the built environment include assessing occupant travel patterns in a museum [12] and in teacher-student-interactions in the classroom [13], [14]. Such implementations are limited, yet growing interest in interaction geography is evident through multiple studies focusing on the movements of building occupants [15–17]. However, tracking movements is an intensive and time-consuming data collection process that uses wearable sensors or camera recordings [12], [17].

This paper presents a time-and-cost efficient approach to exploring building occupant behavior via movements using Virtual Reality (VR) technology. In a pilot study, the authors analyzed the movements of 10 participants in a

virtual museum to examine the extent to which interaction geography further the current understandings of building occupant behavior with the research question:

"What insights can Interaction Geography offer to the understanding of participant behavior in a VR museum?"

The authors, thus, explored movement patterns (obtained via Interaction Geography) to identify how participants interacted with a building setting via real-time data.

2. Literature Review

2.1. Building Occupant Behavior Research

Building occupant behavior is under the influences of environmental, contextual, psychological, physiological, social, time, and random factors (Figure 1) [18]. Lighting, temperature, and indoor air are environmental factors. Building features such as orientation and construction are contextual; gender, age, and occupation are psychological; individual perceptions of temperature are physiological, cultural groups and organizational regulations are social factors [19]. Time-related events (e.g., working shifts) and random movements are influential as well [20]. Studies on building occupant behavior focus on environmental and contextual factors due to their quantifiable nature. For instance, researchers operationalize environmental factors as Indoor Environmental Quality (IEQ) variables that are measurable using satisfaction surveys (e.g., pre-and post-occupancy evaluations) and real-time devices (e.g., light meters, sensors) [21].

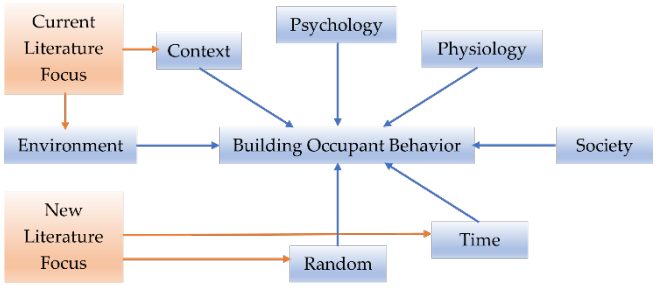

Figure 1: Factors that Influence Building Occupant Behavior

In the typical approach of post-occupancy evaluation (POE), occupants will complete a survey nine to twelve months after moving into a building. The two components that make up POE include (i) subjective perceptions (i.e., comfort and satisfaction) and (ii) physical measurements (i.e., building features) [9]. Both components contain IEQ variables such as temperature, light, noise, privacy, view, decoration, cleanliness, and so on. Occupants use Likert ratings to indicate their subjective perceptions of IEQ variables and their impacts. For example, the Building Use Studies (BUS) survey includes 7-point rating scales (e.g., uncomfortable to comfortable) for 11 IEQ variables (e.g., thermal, acoustic, appearance) [22]. Among IEQ variables, noise, air quality, light, and thermal are most influential to building occupants [1], [23].

Regarding physical measurements, devices like meters and sensors help researchers estimate how IEQ variables might influence building occupants over time. Energy and water consumption plus IEQ variables such as thermal, lighting, air quality, and acoustics make up most of this component [10]. Electricity usage (e.g., applicant loads), window, fan, and air conditioning operation are occupant behaviors of interest within residential and commercial buildings; these studies dominate the corresponding literature [19]. In [18], the authors discussed the current state of building occupant behavior through the following environmental and contextual factors (i.e., IEQ variables): window, lighting, shading, and air conditioning (AC). The focus on this subset of factors/variables is reasonable as professionals (e.g., engineers, architects, designers) and stakeholders (e.g., managers, owners) are concerned with the social and financial costs of energy consumption and life cycle of buildings. The authors in [24] also projected a decline in energy purchasing power of $11,258,2019 by 2099, implying that low-income populations would suffer from the inability to consume energy in response to climate change (i.e., global warming). According to the authors in [25], residential buildings that withstand a wide temperature fluctuation (e.g., from – 20°C to + 30°C) are costly, especially with a deficit in Gross Domestic Product (e.g., – 2% in 2017) due to global warming. Said costs explain why environmental and contextual factors (i.e., IEQ variables) predominate the current state of building occupant behavior research (Figure 1).

Viewing building occupant behavior as stochastic (i.e., random) with the variants between occupants that evolve over time represents a research paradigm shift [15]. Recent additions to POE include visual records, data of building structure/service/system, window sensors, GPS-tracked mobility, and so on [10]. In [6] the authors utilized an agent-based simulation (ABS) model and sensor-based data to predict probabilities of window operation in commercial buildings. This model reduces stochastic uncertainties by cross-referencing multiple IEQ variables like temperature, air, and humidity, in a single behavior: opening a window. However, the ABS model did not take into account the complex occupant interactions in real-world settings and the underlying psychological factors.

2.2. Interaction Geography

Interaction Geography is the comprehensive analysis of audiovisual data of interactions via sociocultural and social lenses [11]. Originating from interaction analysis in Computer Supported Collaborative Learning (CSCL), this approach converts and presents selective subsets of verbal and physical behaviors into transcripts so researchers can comprehend social events from insider perspectives [26]. The transcript is not merely a record of audiovisual data but a portrait that captures the emotions, behaviors, and potential intentions of people who engage in a social event

[27]. Transcripts are vital to interaction analysis, but their production techniques have evolved little over the years. Language-processing software such as Microsoft Word is typically used to produce transcripts that include conversations and gestures or multimodal transcription [28]. Through the "presentation of text," researchers preserve data integrity by not correcting "particulars" or "tiny things" that might reveal the sociocultural backgrounds or underlying thoughts of the event in participants [27], [29].

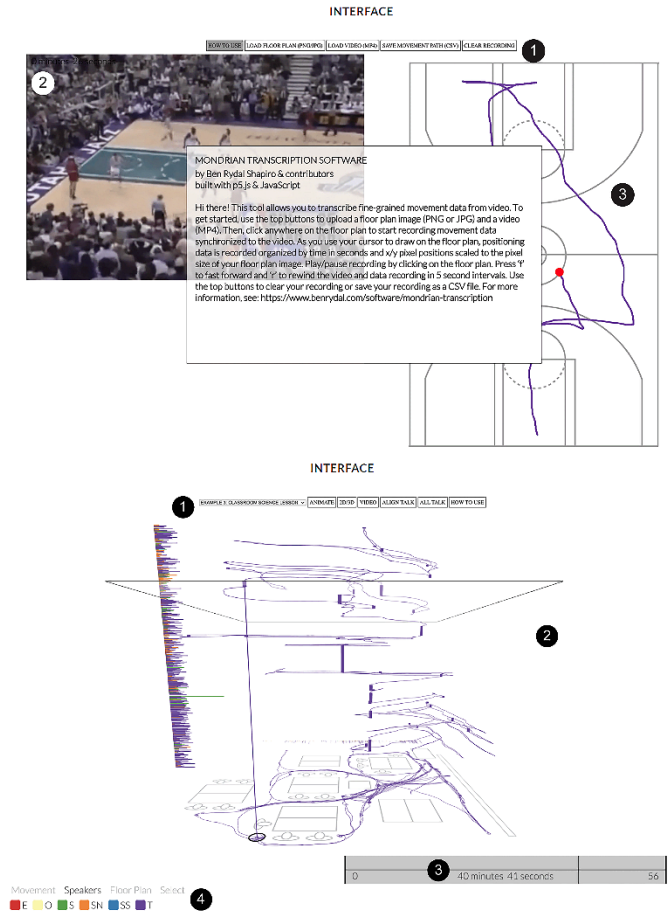

Figure 2: Mondrian Transcription and IGS Interfaces [12]

However, language-based transcription is inadequate to represent the intrinsic complexity of social behaviors. Interaction Geography combines qualitative analysis with time geography (i.e., time-space coordination of human behaviors in social events) to analyze audiovisual data [30], [31]. In [11], the author offered a cutting-edge method for Interaction Geography with two key components (Figure 2). First, via Mondrian Transcription web-based software, the author extracted and encoded participant movements and conversations over space and time from audiovisual data. This process resulted in a spreadsheet containing the pixel positions and movement transcripts of participants. Mondrian Transcription is among the earliest tools that transcribe movements and conversations (i.e., pixel positions and timed verbal exchanges). Second is Interaction Geography Slicer (IGS), a tool that syncs transcripts of movements and conversations with specific time frames in audiovisual data. IGS, therefore, enables exploratory analyses and dynamic visualizations of Mondrian transcription [26].

One application of Interaction Geography in buildings was to study museum visitor traveling patterns [12] and classroom interactions of teachers and students [13]. In [12], the authors analyzed 22 case studies with 72 hours of audio and video recordings of museum visitors to determine their movements, interactions, and technology use. The data illustrated how "visitors' personal and social history, prior knowledge, and relationship to one another" influenced their choice of navigation and experience in a museum setting. In [13], the authors analyzed audiovisual excerpts of teacher-student interactions in two classrooms. Results indicated that the teachers developed repetitive circulation patterns around projector and tables. Their travel patterns also fluctuated during classroom hours, depending on the changes in instructional content. The findings raised concerns regarding how teachers should monitor their classroom movements and interactions to ensure effective teaching. Interaction Geography, thus, is helpful for the stochastic paradigm in building occupant behavior research as it reveals the randomness underlies occupants' behavior across space and time.

3. Methodology

In this paper, the authors proposed a novel application of Interaction Geography in building occupant behavior research using Virtual Reality (VR). Like the authors in [12], we also chose a museum setting to explore occupant behaviors across time and space. VR technology enabled a time- and cost-efficient simulation of a museum and therefore was fundamental for piloting occupant behavior study in the chosen setting.

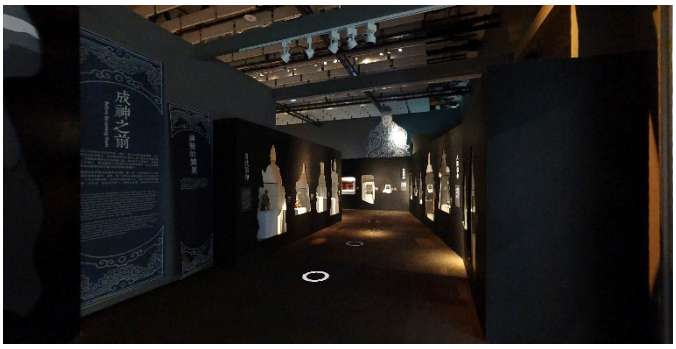

Figure 3: The VR Museum [32] as Seen in a Meta Quest 2 Headset

3.1. VR Museum Session

This pilot study utilized a public VR museum (Figure 3) from the Matterport website (https://matterport.com/) [32]. Participants ($n = 10$) each attended a VR session, which included 10 minutes of training and 20 minutes (or more) of exploring the VR museum. Using Meta Quest 2 headsets, the authors recorded VR sessions (in video and audio) as participants explored the virtual building space.

Using the hand controllers, participants moved through the space by pointing at the white circles on the floor. The participants, however, could not interact with the artifacts (e.g., statues) and spatial elements (e.g., door) in the virtual museum as they are only 360-degree photographs.

3.2. Interaction Geography Transcription

Mondrian Transcription (https://www.benrydal.com/software/mondrian-transcription) [12] helped transcribe recorded movements and interactions into pixel positions on a scale diagram that illustrates space arrangements in a building (i.e., a floor plan). The museum floor plan and the audiovisual recordings of the VR sessions were uploaded to Mondrian Transcription's web-based interface (Figure 4) for manual tracing. Both files were then visible next to each other on a computer screen. By hovering the mouse cursor over the floor plan, the authors displayed a path that followed the participants' movements as shown in the recording. The authors accurately traced the time-specific movements using the keyboard to play, rewind, and pause the recording. Analysis results included a traced floorplan demonstrating a two-dimensional (2-D) movement path and a spreadsheet logging every step of the participant in the space with x- and y-coordinates. The authors repeated this process with all recordings.

Figure 4: Mondrian Transcription's Web-based Interface with Manual Tracing of Participant's Movements

IGS (https://www.benrydal.com/software/igs) [12] was another process the authors used to visualize the traced movement paths of participants over time. We uploaded Mondrian Transcription transcripts (i.e., the spreadsheets with x- and y-coordinates) and the corresponding VR recordings to this web-based interface. IGS synchronized all movements and conversations of each participant following a timeline that equaled the length of each recording. This process resulted in an animated floor plan illustrating the 2-D movement path over a corresponding three-dimensional (3-D) conversation timeline. Hovering the cursor on top of the animated floor plan allowed the authors to rewind and analyze participant movements and conversations at a specific point in time.

4. Results

Participants ($n = 10$) in this pilot study were all college students in the 18 – 34 age group, with 67 % female and 33 % male. This was a convenient sample of volunteers who dedicated their time to participate in this study without compensation. Table 1 summarizes the demographics and logistics of all participants.

Table 1: Demographics and Logistics of Participants

ID No.	Time in VR	Use VR	Major
P_1	12 minutes	Monthly	Design
P_2	15 minutes	Yearly	Design
P_3	20 minutes	Never	Design
P_4	28 minutes	Never	Non-design
P_5	17 minutes	Never	Non-design
P_6	14 minutes	Never	Non-design
P_7	14 minutes	Never	Non-design
P_8	12 minutes	Never	Non-design
P_9	30 minutes	Never	Design
P_10	12 minutes	Monthly	Design

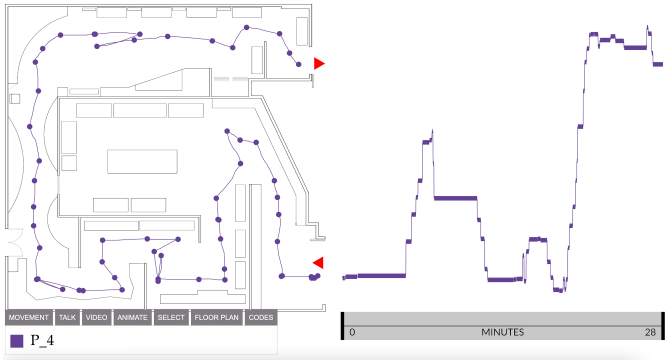

Figure 5: Floor plan of the VR museum with the Traced Movements Across Time and Space of a Participant

4.1. Participant Behavior in a Virtual Space

Most participants (70%) had minimal prior exposure to VR technology, and the average time they spent exploring the virtual museum was around 17 minutes. Participants all completed the VR session from start to finish. The floor plan (Figure 5) indicates the entrance (i.e., the upper red arrow) and the exit (i.e., the lower red arrow), with representations of objects (i.e., artifacts), display cases, and furniture in the VR museum. Although the white circles predetermined the VR museum navigation, participants were free to skip circles, come back, and stay for a certain amount of time at specific points. Such behaviors reflected how participants behaved in the VR museum regarding the space arrangement (e.g., whether display cases with the artifacts captured participant attention as planned by the interior designer). Figure 5 below illustrates the fourth participant's (P_4) movements across space and time. P_4's travel path is depicted on the museum floor plan, and the adjacent timeline displays the periods they spent in each area of the space throughout their recording. For 28 minutes, P_4 (a non-design major) traveled across the VR museum yet entirely skipped the central exhibition with multiple display cases and artifacts. This observation

is one of the behavior discrepancies among participants. The section below summarizes notable findings from the movements across space and time of all participants in this pilot study. Instead of discussing the movements across space and time of each participant, the authors stacked the travel paths of those with the same background (i.e., design vs. non-design) together for a better comparison.

4.2. Movement Density and Personal Background

The authors analyzed all the transcripts and organized them into two categories based on movement density: design and non-design major participants. To give a comprehensive view of the results, the authors overlaid the traced paths of participants together on the floor plan for each category. Figure 6 depicts the paths of five participants who major in design (P_1, P_2, P_3, P_9, and P_10).

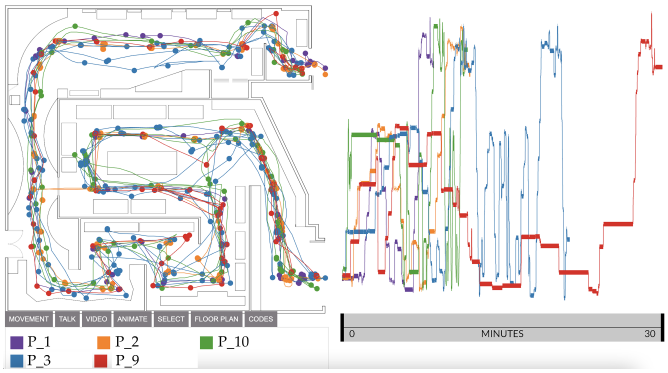

Figure 6: Overlays of Movements Across Time and Space of Design Participants

- Design-major participants had intense movement density; as shown in Figure 6, these participants spent more time at the entrance and exit (as shown in multiple traced points). They also returned to specific spots (as their paths overlapped several times). None of them skipped the central exhibition, and all followed the intended design of the floor plan.
- P_2 discovered the door that led directly to the central exhibition while exploring the lower part of the central exhibition. P_2 then crossed the door to a hallway previously visited and went back to the central exhibition to complete the upper part (the orange path in Figure 6). Notably, P_2 indicated only yearly use of VR, which is less prior experience than P_1 and P_10 indicated. The other participants all navigated from the entrance toward the long hallway leading to the central exhibition and ended at the exit.
- The synchronized timeline on the right of Figure 6 also reveals time durations spent throughout the VR museum. P_1 and P_3, for example, spent more time exploring at the beginning (about one-fourth and one-half of their time, respectively) but later skimmed through the space. Meanwhile, P_2, P_9, and P_10 divided their time more evenly across the VR museum.

Figure 7 illustrates the paths of five participants who were in non-design majors (P_4., P_5, P_6, P_7, and P_8). Their behavior showed some differences compared to their design counterparts.

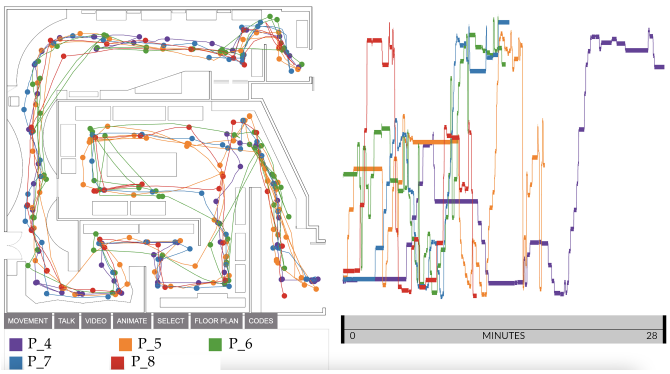

Figure 7: Overlays of Movements Across Time and Space of Non-design Participants

- The movement density was less condensed for non-design participants. Figure 7 shows that non-design participants spent equal time throughout the VR museum (i.e., as shown in the straightforward and less-overlapped paths). P_4, as a notable case, even skipped the central exhibition altogether (Figure 5). Especially, no participant ever noticed the door connecting the hallway and the central exhibition.
- The traced paths also differed from one participant to another. For instance, P_4 had the most straightforward path that started at the entrance and flowed through the hallway to the exit. P_5, on the contrary, explored the VR museum twice using the same path. P_6 repeatedly visited the upper left curved display in the hallway, the left upper corner display cases in the central exhibition, and three display cases at the end of the museum (as shown in the overlaps in the green traced path). P_7 showed a similar travel path to those of the design participants (i.e., following the intended navigation of the floor plan) yet visited each spot only once. P_8 revisited the first half of the VR museum yet skimmed through the last half. This participant also explored the central exhibition counterclockwise, thus, differing from the rest. It's worth noting that all non-design participants had never used VR technology before.
- The synchronized timeline on the right of Figure 7 also reveals time durations spent in the VR museum. P_4 and P_5, for instance, spent more time exploring at the beginning (about one-half of their time) and moved faster at the end. P_6, P_7, and P_8 divided their time into small durations evenly spanned over the exploration.

5. Conclusion

Participants all finished the VR museum with an average time of 17 minutes from start to finish, except P_4,

who skipped the central exhibition. Prior experience in VR technology, therefore, was not an influential factor in participant behavior. Similar to the authors in [12], this pilot study also found that "personal history" and "prior knowledge" (i.e., design vs. non-design majors) affected how participants navigated and experienced the virtual museum.

First, design-major participants explored the space more thoroughly than their non-design counterparts. They also spent extended time at the entrance and exit, where there were artifacts, signs, and display cases; revisited specific spots; and examined the central exhibition equally as the hallway. P_2 even found the door leading directly to the central exhibition, possibly due to their design knowledge (i.e., the psychological factor of occupation) which helped them navigate and engage with the space more effectively. The non-design participants paid less attention to the space, as evidenced by their behavior: for example, they did not go back to check artifacts and display cases along the paths, and P_4 skipped the central exhibition altogether. Said behaviors raise concerns about whether all occupants perceived space design intentions equally.

Second, either design or non-design participants explored the VR museum at their own pace. Some spent more time in the beginning and rushed at the end; others spent equal time periods in the whole space. This observation shows an underlying social factor relating to personal interests and connection to certain artifacts or display cases. The degree of personal interest one has with the space might affect their behaviors [12].

One limitation of this pilot study is that each participant explored the VR museum independently, which does not account for social interactions between them. Moreover, the VR museum is a 360-degree-captured environment or a compilation of multiple 2-D images of a real space. Participants could not interact with artifacts, display cases, and furniture. Future research will use an interactive VR environment so that participants can interact with the objects in their surroundings. The authors hope to gain further insights into occupant behavior via Interaction Geography and more sophisticated VR technology.

Conflict of Interest

The authors declare no conflict of interest.

Acknowledgment

The authors thank James Amann and the student workers at the Creative Media Industries Institute, Georgia State University for their hospitality and support. This study is supported by the 2022 Summer Research Fund for faculty from Welch School of Art and Design, College of the Arts, Georgia State University.

References

[1] L. T. Graham, T. Parkinson, S. Schiavon, "Lessons learned from 20 years of CBE's occupant surveys", *Buildings and Cities*, vol. 2, no. 1, pp. 166–184, 2021. http://doi.org/10.5334/bc.76

[2] C. D. Roa, S. Schiavon, T. Parkinson, "Targeted occupant surveys: A novel method to effectively relate occupant feedback with environmental conditions", *Building and Environment*, pp. 107129, 2020. https://doi.org/10.1016/j.buildenv.2020.107129

[3] K. A. Young, "Direct from the source: the value of'think-aloud'data in understanding learning", *Journal of Educational Enquiry*, 2005. http://hdl.handle.net/10453/6348

[4] C. D. Darker, D. P. French, "What sense do people make of a theory of planned behaviour questionnaire? A think-aloud study", *Journal of health psychology*, vol. 14, no. 7, pp. 861–871, 2009. https://doi.org/10.1177/1359105309340983

[5] C. Macal, M. North, "Introductory tutorial: Agent-based modeling and simulation", *Proceedings of the winter simulation conference 2014*, pp. 6–20, 2014. https://doi.org/10.1109/WSC.2014.7019874.

[6] M. Jia et al., "A systematic development and validation approach to a novel agent-based modeling of occupant behaviors in commercial buildings", *Energy and Buildings*, vol. 199, pp. 352–367, 2019. https://doi.org/10.1016/j.enbuild.2019.07.009

[7] S. Norouziasl, A. Jafari, C. Wang, "An agent-based simulation of occupancy schedule in office buildings", *Building and Environment*, vol. 186, pp. 107352, 2020. https://doi.org/10.1016/j.buildenv.2020.107352

[8] K. R. Rozo et al., "Modelling building emergency evacuation plans considering the dynamic behaviour of pedestrians using agent-based simulation", *Safety science*, vol. 113, pp. 276–284, 2019. https://doi.org/10.1016/j.ssci.2018.11.028

[9] P. Li, T. M. Froese, G. Brager, "Post-occupancy evaluation: State-of-the-art analysis and state-of-the-practice review", *Building and Environment*, vol. 133, pp. 187–202, 2018. https://doi.org/10.1016/j.buildenv.2018.02.024

[10] D. Sanchez Leitner, N. Christine Sotsek, A. de Paula Lacerda Santos, "Postoccupancy evaluation in buildings: Systematic literature review", *Journal of Performance of Constructed Facilities*, vol. 34, no. 1, pp. 03119002, 2020. . https://doi.org/10.1061/(asce)cf.1943-5509.0001389

[11] B. R. Shapiro, "What About Interaction Geography to Evaluate Physical Learning Spaces?", *Teacher Transition into Innovative Learning Environments*, pp. 167–179, 2021. https://doi.org/10.1007/978-981-15-7497-9_14

[12] B. R. Shapiro, R. P. Hall, D. A. Owens, "Developing & using interaction geography in a museum", *International Journal of Computer-Supported Collaborative Learning*, vol. 12, no. 4, pp. 377–399, 2017. https://doi.org/10.1007/s11412-017-9264-8

[13] B. R. Shapiro, B. Garner, "Classroom interaction geography: visualizing space & time in classroom interaction", *Journal of Research on Technology in Education*, pp. 1–15, 2021. https://doi.org/10.1080/15391523.2021.1927265

[14] G. Fernandez-Nieto et al., "Classroom Dandelions: Visualising Participant Position, Trajectory and Body Orientation Augments Teachers' Sensemaking", *CHI Conference on Human Factors in Computing Systems*, pp. 1–17, 2022. https://doi.org/10.1145/3491102.3517736

[15] S. Carlucci et al., "Modeling occupant behavior in buildings", *Building and Environment*, vol. 174, pp. 106768, 2020. https://doi.org/10.1016/j.buildenv.2020.106768

[16] M. Arslan, C. Cruz, D. Ginhac, "Understanding occupant behaviors in dynamic environments using OBiDE framework", *Building and environment*, vol. 166, pp. 106412, 2019. https://doi.org/10.1016/j.buildenv.2019.106412

[17] N. Haidar et al., "Towards a new graph-based occupant behavior modeling in smart building", *2019 15th International Wireless Communications & Mobile Computing Conference (IWCMC)*, pp. 1809–1814, 2019. https://doi.org/10.1109/IWCMC.2019.8766569

[18] F. Stazi, F. Naspi, M. D'Orazio, "A literature review on driving factors and contextual events influencing occupants' behaviours in buildings", *Building and Environment*, vol. 118, pp. 40–66, 2017. https://doi.org/10.1016/j.buildenv.2017.03.021

[19] E. Delzendeh et al., "The impact of occupants' behaviours on building energy analysis: A research review", *Renewable and sustainable energy reviews*, vol. 80, pp. 1061–1071, 2017. https://doi.org/10.1016/j.rser.2017.05.264

[20] S. Chen et al., "The impacts of occupant behavior on building energy consumption: A review", *Sustainable Energy Technologies and Assessments*, vol. 45, pp. 101212, 2021. https://doi.org/10.1016/j.seta.2021.101212

[21] C. Shen, K. Zhao, J. Ge, "An overview of the green building performance database", *Journal of Engineering*, vol. 2020, 2020. https://doi.org/10.1155/2020/3780595

[22] Arup, "BUS methodology." https://busmethodology.org.uk/ . (accessed: 05-Oct-2021).

[23] I. A. Sakellaris et al., "Perceived indoor environment and occupants' comfort in European "modern" office buildings: The OFFICAIR study", *International journal of environmental research and public health*, vol. 13, no. 5, pp. 444, 2016. https://doi.org/10.3390/ijerph13050444

[24] A. Rode et al., "Estimating a social cost of carbon for global energy consumption", *Nature*, vol. 598, no. 7880, pp. 308–314, 2021. https://doi.org/10.1038/s41586-021-03883-8

[25] N. Stern, J. E. Stiglitz, *The social cost of carbon, risk, distribution, market failures: An alternative approach*, vol. 15, , National Bureau of Economic Research Cambridge, MA, USA, 2021. https://files.static-nzz.ch/2021/4/26/7e32b21f-81b9-4033-907c-7aaeba85e7a5.pdf

[26] A. Mathur, B. R. Shapiro, "Interactive Transcription Techniques for Interaction Analysis", *16th International Conference of the Learning Sciences (ICLS)*, pg. 19-26, 2022. https://scholarworks.gsu.edu/ltd_facpub/46

[27] A. Hepburn, G. B. Bolden, *Transcribing for social research*, Sage, 2017.

[28] J. Bezemer, D. Mavers, "Multimodal transcription as academic practice: A social semiotic perspective", *International Journal of Social Research Methodology*, vol. 14, no. 3, pp. 191–206, 2011. https://doi.org/10.1080/13645579.2011.563616

[29] G. Jefferson, "Glossary of transcript symbols with an introduction", *Pragmatics and Beyond New Series*, vol. 125, pp. 13–34, 2004.

[30] T. Hägerstrand, "Reflections on "what about people in regional science?"", *Papers of the Regional Science Association*, vol. 66, no. 1, pp. 1–6, 1989. https://doi.org/10.1007/BF01954291

[31] B. Jordan, A. Henderson, "Interaction analysis: Foundations and practice", *The journal of the learning sciences*, vol. 4, no. 1, pp. 39–103, 1995. https://doi.org/10.1207/s15327809jls0401_2

[32] Matterport Inc., "Matterport." https://matterport.com/ . (accessed: 03-Sep-2022).

Dr. Hoa Vo is an Assistant professor in Interior Design at the Welch School of Art and Design, College of the Arts, Georgia State University. She earned her Ph.D. degree in Interior Design from the University of Minnesota in 2021.

Her research covers adaptive technologies (AR, VR, digital modeling and fabrication) in teaching, intersectional collaborations in design, creativity and feedback practices in design, and physical experiences in the built environment. She has published in Journal of Creativity (JOC), Sustainability of MDPI, International Journal of Designs for Learning (IJDL), Archnet-IJAR: International Journal of Architectural Research, Academic Exchange Quarterly (AEQ), and multiple peer-reviewed conference proceedings.

Peter Huesemann-Odom is a M.F.A. candidate in Interior Design (expecting 2024) at the Welch School of Art and Design, College of the Arts, Georgia State University. With over fifteen years working in creative departments and a Bachelor of Arts degree in business administration, he consults, supports, as well as inspires design aesthetics worldwide.

He lived in Brazil, Germany, Sweden, and now the States to research how much space we need to live a happy life, what we define as "home," and how consumers will shop in the future.

JENRS

Received: 18 June 2022, Revised: 23 September 2022, Accepted: 29 October 2022, Online: 27 November 2022

DOI: https://dx.doi.org/10.55708/js0111002

Real-Time Acquisition and Classification of Electrocardiogram Signal

Sheikh Md. Rabiul Islam[1,*], Akram Hossain[2], Asif Abdullah[3]

[1]Department of Electronic and Communication Engineering, Khulna University of Engineering & Technology, Khulna,9203, Bangladesh
[2]Department of Biomedical Engineering, Khulna University of Engineering & Technology, Khulna,9203, Bangladesh
[3]Department of Biomedical Engineering, Jashore University of Science and Technology, Jashore, 7408, Bangladesh
*Corresponding author: Sheikh Md. Rabiul Islam, Dept. of ECE, KUET, +8801714087378, & Email: robi@ece.kuet.ac.bd

ABSTRACT: Cardiovascular disease (CVD) is the leading cause of death. The transition in cardiovascular disease threatens the economies of the less developed world. An electrocardiogram (ECG) machine is a device that checks the patient's heart rhythm and electrical activity. ECG signals give crucial information about the heart and numerous cardiac problems, such as coronary artery disease, myocardial infarction, and hypertension, which can be detected with an ECG report. The success rate for cardiac disease diagnosis will rise if ECG signals can be adequately recognized and interpreted. Classic signal processing and machine learning algorithms are utilized to evaluate the ECG signal and detect distinct types of arrhythmia for early treatment and prevention of cardiovascular diseases. To provide a sustainable solution for developing countries, we need to make an accurate diagnosis device that is portable and low-cost. This research aims to create a new low-cost ECG device and interface patients with HealthyPi v3 which is a miniature raspberry pi-based vital sign monitor to record raw ECG signals. We proposed an integrated environment with classical ECG acquisition and classification techniques to obtain the preferable outcome. Also, we allowed us to assimilate with a mobile remote monitoring system to create a dynamic healthcare monitoring environment for the patients. This work implies the acquisition of real-time ECG data via HealthyPi V3 integrated with peripheral capillary oxygen saturation (SpO2) sensor and temperature sensor. The software is designed to read and analyze the hardware system-driven real-time ECG data, heart rate, blood pressure, respiratory rate, and temperature. To categorize the QRS complex of ECG data obtained and analyzed by the hardware-software system for heart disease prediction, Support Vector Machine (SVM) classifier, Convolutional Neural Network (CNN), and Recurrent Neural Network (RNN) is applied where CNN has achieved the highest accuracy while processing the signal.

KEYWORDS: Real-time ECG Monitoring, HealthyPi V3, Machine Learning, SVM, CNN, RNN

1. Introduction

Every day, a considerable number of biomedical data is generated to monitor and observe the physiological status of the human body as a result of rapid technological developments and the rising use of portable monitoring devices. The physiological activity of organs, including the heart, brain, muscles, cornea, and others, is measured using these biological signals. One or more electrodes are frequently placed on the organ of interest to obtain them. The most frequent physiological signals collected from the heart and brain are the electrocardiogram and electroencephalogram (EEG), respectively.

Electrocardiography, also known as ECG or EKG, is the process of creating an electrocardiogram. It's a graph of the voltage versus time of the heart's electrical activity using electrodes on the skin. During each cardiac cycle, these electrodes detect the tiny electrical changes that occur due to cardiac muscle depolarization and repolarization. Several cardiac problems cause changes in the typical ECG pattern, including cardiac rhythm disturbances like atrial fibrillation and ventricular tachycardia, insufficient coronary artery blood flow such as myocardial ischemia and infarction, and electrolyte imbalances.

Diseases like these can be interpreted using ECG, making it a simple solution for a primary diagnosis of heart problems. Signals must be processed before they can be interpreted. A noisy raw signal can make it difficult to decipher the signal's meaning. Different noise removal approaches have been implemented to remove this noise from ECG [1].

Einthoven pioneered the use of the electrocardiogram in clinical practice more than a century ago. It's a linear recording of the heart's electrical activity that's been time-stamped for each cardiac cycle; an atrial depolarization wave (P wave), ventricular depolarization wave (QRS complex), and ventricular repolarization wave (T wave) are recorded in succession (Figure 1) [2]. The shape of these individual waves changes as they are recorded from various locations (leads). In either case, the order is always P–QRS–T.

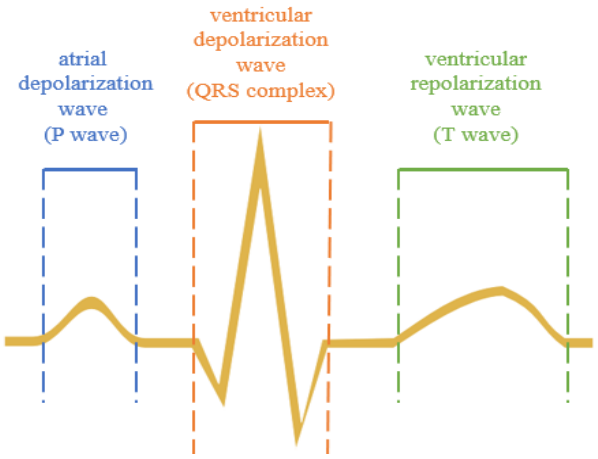

Figure 1: Recorded ECG signal depicting P wave, QRS complex, T wave

While the three-lead ECG proved a valuable tool for detecting arrhythmias, it was quickly discovered that there were "silent zones" in the heart where a myocardial infarction may go undetected [3]. In 1934, Dr. Frank N. Wilson of the University of Michigan coined the phrase "central terminal." Connecting the three limb electrodes established a central negative lead reflecting a 'ground' or reference terminal. The potential difference between that spot on the body and what might be thought of as zero was detected using an electrode from the body surface linked to this ground using a galvanometer. These 'unipolar' leads were not the same as 'bipolar' leads, which assess the difference in potential between two places on the body surface.

There are two remote heart monitoring device options: "on-site" and "off-site." On-site monitoring eliminates the need to send the patient's heart signal to a remote location for processing. On the other hand, the acquired cardiac signal must be sent to a remote site over WiFi or GSM [4]. During the integration, patients can get real-time remote monitoring and analysis of their ECG data. The cohesive transferable system allows wireless data transfer [5]. A non-intrusive, lightweight ECG monitoring equipment is essential for cardiac patients.

HealthyPi is a fully functional, open-source vital sign monitor. The HealthyPi add-on HAT (hardware attached on top) uses the Raspberry Pi as its compute and display platform, transforming it into a powerful sign-monitoring system [6]. It is the best and most recent solution for coronary disease. A sensor node is affixed to the patient's skin to do this. Sensor nodes respond to even minor voltage variations and provide a precise and trustworthy assessment of cardiovascular status [7].

This study used a two-dimensional (2D) deep convolutional neural network to classify ECG signals. The most well-known and often-used algorithm is CNN. CNN has a structure akin to a traditional neural network modeled after the neurons found in human and animal brains. More specifically, the visual cortex of a cat's brain is made up of an intricate pattern of cells, and the CNN simulates this pattern [8]. The short-time Fourier transform was used to first convert the time-domain ECG signals into time-frequency spectrograms, which represent the five different types of heartbeats: average beat (NOR), left bundle branch block beat (LBB), right bundle branch beat (RBB), premature ventricular contraction beat (PVC), and atrial premature contraction beat (APC). Finally, the ECG arrhythmia types were detected and categorized using the spectrograms of the five arrhythmia kinds as input to the 2D-CNN. The primary benefit of CNN over its forerunners is that it finds significant features automatically and without human supervision, making it the most popular. RNN is not thought to be as powerful as CNN. When compared to CNN, RNN has less feature compatibility [9].

When classifying various data clusters, the Support Vector Machine is employed as a training method. The algorithm underlies this classification strategy and looks for the best separation surface [10]. Finding a hyperplane that can divide data clusters so that the distance between the mean of the data points and the hyperplane is as little as possible is the classifier's goal. SVM has often known as a maximum marginal classifier [11]. Due to its convex optimization problem, it has good generalization performance for high-dimensional data. The most used method is SVM. This is because it performs more generally for different types of data than algorithms like ANN, which have the issue of locally minimal solutions. Researchers have widely utilized SVM as a classification approach for ECG data [12-14].

Based on morphological and temporal data, a recurrent neural network is used to study the fundamental characteristics of ECG beats. Active learning is used to pick the most instructive beats and add them to the training set to increase system performance when new samples are collected. As the training set expands, the system is updated [15]. RNN instantly picks up on the subtle changes between samples from various classes. The recurrent connections enable a memory of past inputs to survive in the internal state of the network at every time step, which can subsequently be exploited to

affect the final network output. The relative position and form of ECG waves can identify several kinds of ECG beats as a time and sequence. Regarding processing, the ECG beats can be categorized by looking at the relationship between time coordinates and signal point amplitudes. Due to the high correlation between ECG signal locations, it makes sense to use RNN in ECG beat categorization.

Many academics have been working on automated heart disease diagnosis for decades. Because it is a typical publicly available arrhythmia database, most of them used the MIT-BIH datasets. It's a freely available dataset that includes reference materials for investigating heart arrhythmia detection according to industry standards, which has been used for basic research and the creation of medical devices since 1980. Many studies rely on handmade or manual feature extraction approaches exploiting the morphological characteristics and time-varying dynamics of ECG as one of the two primary phases in a conventional machine learning-based classification issue, namely feature extraction and classification [16]. Manual descriptions used a Kalman filter and Bayesian filtering strategy for high-accuracy classification, but it was confined to only two classes, i.e., binary classification. However, the accuracy and classification attained a beat-by-beat analysis technique with a class-oriented framework and an SVM classifier using Hermite transform coefficients [17, 18].

2. Materials and Methods

The principal flow diagrams of this research have shown in Figure 2. This work implemented a hardware and software module to create an interface between the patient and the device for collecting the ECG data from the patient. A computer, a Raspberry Pi, a HealthyPi v3 equipped with an ECG module, a Spo2 sensor, a temperature sensor, electrodes, and software platforms written in Python and Java have been used to construct the system. Later, to develop GUIs and do signal processing and categorization, Python was employed.

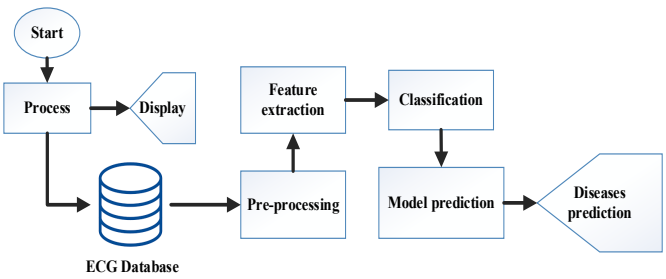

Figure 2: Flow chart of ECG Signal Acquisition and Classification.

2.1. Data Acquisition

Raspberry Pi and the HealthyPi v3 module were used to collect data on the patient skin. This device employed three electrodes, as shown in Figure 2. The module was an interface, and the Raspberry Pi was the host microcontroller. A Raspberry Pi HAT called the HealthyPi v3 can also be used as a stand-alone device for medical diagnosis and treatment. With its mobility, Wi-Fi, and wearable characteristics, the third iteration of HealthyPi sets new standards in totally accessible health solutions. The device was used to assess real-time electrocardiogram data, heart rate, heart-rate variability, and breathing based on impedance pneumography, pulse oximetry, and body temperature.

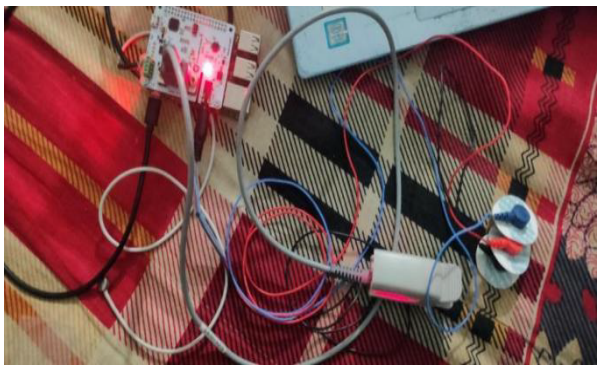

Figure 3: Connected HealthyPi v3 with Raspberry Pi and corresponding electrodes.

The shield comes with a 3-electrode cable and a standard stereo jack for connecting the electrodes to the board. The electrode connector's other end would connect to body-attached Snap-on electrodes [19].

The Module was attached to a Raspberry Pi and used to interface with the human body. The data was taken in the Biomedical Signal Processing Laboratory, Dept. of Biomedical Engineering, Khulna University of Engineering & Technology. This department approved the ethical issues.

2.2. Preprocessing

The suggested system's power line noise distorts the recorded ECG data. The ECG signals' integrity is compromised by these aberrations, making interpreting them more difficult. Even though the amplifiers employed in biomedical signal processing have a high common-mode rejection ratio (CMRR), residual Power Line Interference (PLI) noise frequently degrades ECG recordings [20]. We utilized a Bandpass filter to reduce noise from the raw ECG data. Band Pass Filters filter or isolate specific frequencies within a typical frequency band. We considered that the filter's center frequency is 0, which determines the frequency band's location and bandwidth. As the filter gets bigger, the frequency band it covers expands. At least two control parameters are usually present in bandpass filters: one for bandwidth modification and another for band position adjustment.

On the other hand, we have also used different filters to filter the raw ECG signal, such as the Moving Average Filter (MA) [21]. The MA filter is a standard FIR (Finite Impulse Response) filter for smoothing an array of

sampled data or signals. It averages M input samples simultaneously to create a single output point.

1) It accepts M input points, computes their average, and outputs a single output point.
2) The filter introduces a certain level of delay due to the computations/calculations involved.

The Low Pass Filter function of the filter has a low-frequency domain response but a strong time domain response.

2.3. Feature extractions from ECG Signal

The process of peak detection was used to extract features. The Hamilton segment and window method were used to detect peaks. The signal is then divided using the R-peak value. Because we needed at least two ECG beats to compute separate intervals, we chose two peaks for a single segment. The remaining ECG peaks are then determined or found using the window technique. The window index falls between -90 and -10 of the R-peak value, with P standing for the highest value. Q is the lowest value in the -40 to -10 range, and T is the highest in the +25-to-+90-degree range. The wavelet component trains the model and QRS complexes. Discrete Wavelet Transform (DWT) has proven to be a valuable technique for detecting peaks. The DWT employs scale and position values based on two powers, which is the most evident distinction. Signal decomposition and reconstruction are the main concerns in DWT and inverse DWT, respectively. Low-pass and high-pass filtering with down sampling and up sampling are the essential concepts of decomposition and reconstruction. We obtained PR and RR intervals by detecting the rest of the peak.

To determine heart rate and blood pressure, the patient and the HealthyPi device were both directly connected to the respiratory, cardiac, and temperature sensors. The Java Environment was then used to capture the data. The plotter was used to create a serial data plot (Figure 6). We first made a user interface using a processing plotter. The changes in blood volume, oxygen saturation, and ECG were graphed in real-time. We created a function that enables us to save the collected data as an a.csv file in JAVA GUI; the data collected by the healthy Pi v3 was visualized.

2.4. Filtering the Data

Residual Power Line Interference (PLI) noise typically impairs ECG recordings, even though the amplifiers used in biomedical signal processing have a high CMRR. These aberrations harm the integrity of the ECG signals, making them harder to interpret. Thus, a bandpass filter was designed to filter the data.

This work also attempted to use a different technique, a MA filter, to smooth the signal. Due to its ease of use and understanding, the Moving Average filter is the most used one in Digital signal Processing (DSP). The MA filter, despite being straightforward, is useful for a typical task: reducing random noise while keeping a distinct step response. Of all the available linear filters, the moving average produces a minor noise for a given edge sharpness. The square root of the number of averaged points yields the noise reduction amount. For instance, a 100-point moving average filter decreases noise by ten.

2.5. Classification

SVM, CNN, and RNN algorithms were used to classify the obtained ECG data. A Python Django application was developed. This program accepts a file as input and segments the raw ECG data into ECG beats before displaying it. After segmentation, it provides examples of the various beat kinds.

To distinguish normal and pathological beats in an ECG, recurrent neural networks were used. The main goal of this research was to make it possible to distinguish between regular and irregular beats automatically. The beat classification performance is classified using the MIT-BIH Arrhythmia Database. A large volume of standard data, such as ECG time series, is employed as inputs to the Long Short-Term Memory Network. The raw ECG dataset was separated into training and testing sub-data. The efficacy, accuracy, and capability of the technique for ECG arrhythmia identification have been proved, as well as quantitative comparisons with several RNN models.

3. Results and Discussion

The signal was collected at 20 fps speed and showed standard stability, as shown in Figure 4.

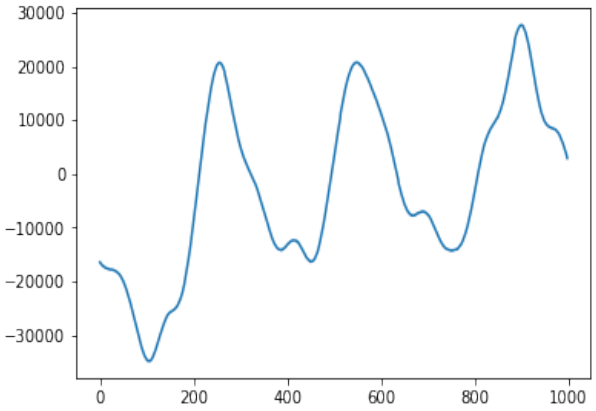

Figure 4: Collected Signal at 20 FPS speed.

The data was then visualized using the Java environment. Serial data were plotted using the plotter,

as shown in Figure 4. The data showed mild distortion, which was further removed by filtering the data. The acquired data was stored as a CSV file. Fig. 5 shows the GUI. The GUI method enables to the opening of a command or function on devices by clicking or pointing to a tiny picture, known as an icon or widget, such as tabs, buttons, scroll bars, menus, icons, pointers, and windows.

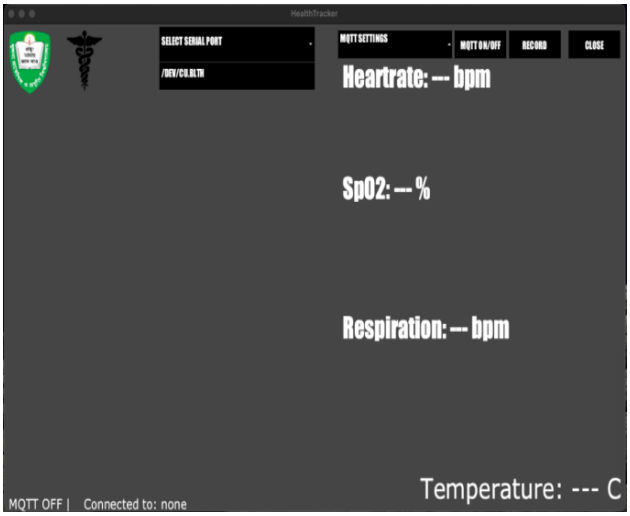

Figure 5: GUI for real-time data acquisition.

The acquired ECG, SpO2, and temperature data were plotted on a graph where the y-axis refers to amplitude, and the x-axis designates time. The graph shows the collected data for 5000 ms, and the highest amplitude obtained is 1 mv. The data showed fluctuation due to external noise and other cofactors related to the acquisition of the signal.

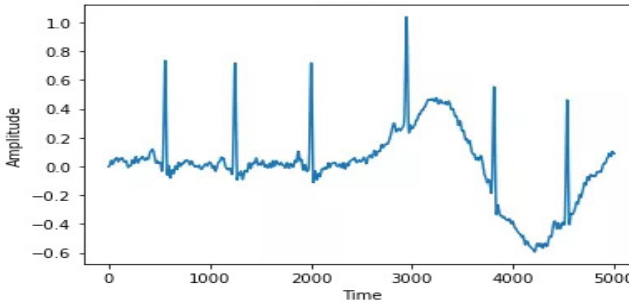

Figure 6: Acquire data of ECG, SpO2, and temperature from the HealthyPi module using Java GUI over the millisecond

The FIR bandpass filter smoothens the obtained signal (Figure 7). As the signal was obtained by one standard lead system, the highest amplitude obtained after filtering the signal equals 0.6 mv, which is standard for one standard lead system data acquisition of ECG signal.

Hamilton Segmenter and the window approach were employed for peak detection, and R peak was effectively discovered. For the training model and QRS complex, we used discrete wavelet components. The heartbeat was retrieved from the signal in this case, Figure 8. The template is shown in a magenta colour. The derived maximum amplitude before and after filtering the signal was 1 mV and 0.6 mV, respectively, as shown in Figures 6 and 7. The amplitude of the signal shown in the template was 0.6 mV. The heart rate was measured by analyzing the characteristics of the obtained ECG signal, and it was found that the heart rate varied within the range of 68-85 bpm for a 4s time span.

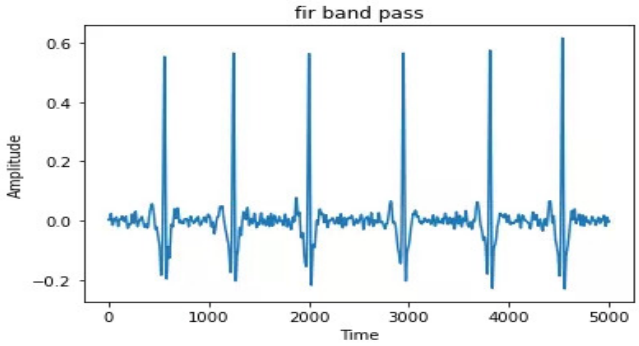

Figure 7: Filtered signal using FIR Band Pass Filter

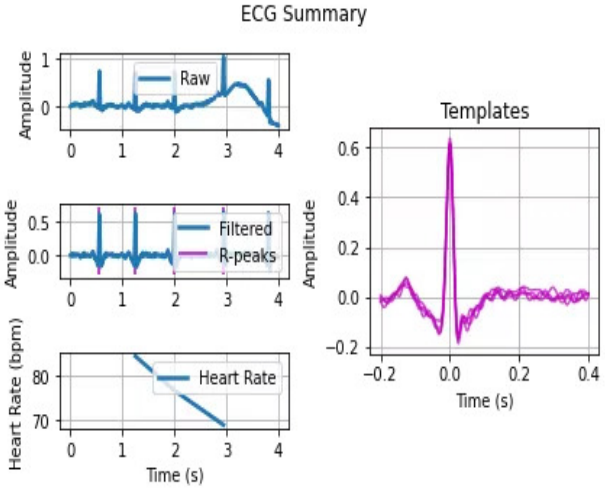

Figure 8: ECG summary and heart rate calculation.

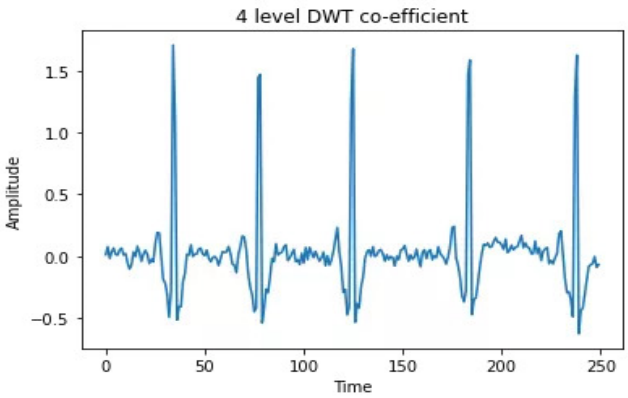

Figure 9: After using 4-level DWT co-efficient.

After restricting heartbeat with Hamilton Segmenter, we employed four-level DWT. Figure 9 shows a DWT that divides a signal into many sets, each with a group of coefficients that characterize the signal's time evolution

in the associated frequency band. A discrete wavelet transform decomposes a signal into several sets, each containing a time series of coefficients describing the signal's time evolution in the corresponding frequency band.

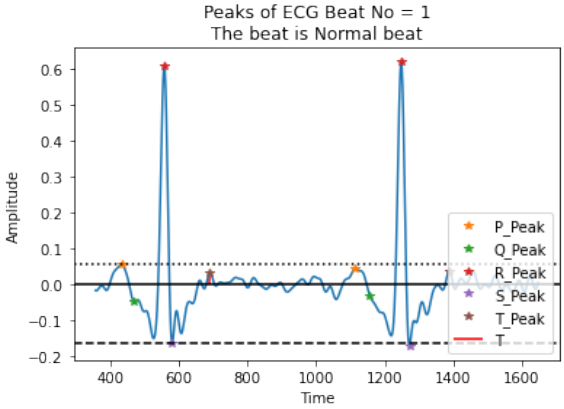

Figure 10: The detected peak of the signal with prediction.

The detected peaks are classified using SVM, CNN, and RNN algorithms [22, 23]. The feature classification is shown in Figure 11, and the results of the classification performance are depicted in the Table. The result shows that the accuracy of detection using the RNN classifier is 95.62%, the CNN classifier is 96.56%, and the SVM classifier is 94.16%. From the table, CNN has shown the highest accuracy.

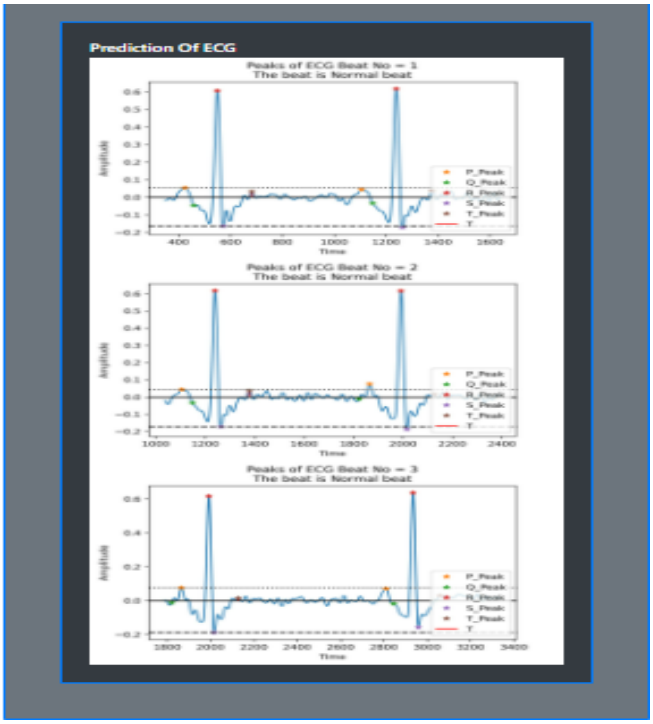

Figure 11: Application for Classification of ECG Signal.

4. Conclusion

This study constructed a system for capturing ECG signals using the HealthyPi module in conjunction with Java script software and users. The majority of the researchers in their study used lead 12. However, we used the ensemble learning boosting strategy with two different classifiers and the lead two signals.

Table 1: Summary of the classification using different machine learning approaches.

Features methods	**Lead**	**Number of ECG beat for training purpose**	**Classifier**	**Classification performance (%)**
Hamilton Segmenter and the window approach	Lead II: R peaks detection, ECG polynomial fitting, ST detection	ECG data sets by the proposed system (Normal: 615 patients *RBBB: 9 patients *LBBB: 32 patients Sinus Bradycardia (SB): 24 patients Atrial Fibrillation (AF): 17 patients ST segment: 6 patients *Critical Beat 1: 26 patients *Critical Beat 2: 3 patients)	RNN Training Data (75%) Testing Data (25%)	95.62%
Hamilton Segmenter and the window approach	Lead II: R-Peak detection, P-Peak detection, Q-Peak detection, S-Peak detection, T-Peak detection		CNN Training Data (75%) Testing Data (25%)	96.56%
Hamilton Segmenter and the window approach, 4-level DWT co-efficient detection, Lyapunov exponent	Lead II: R-Peak detection, P-Peak detection, Q-Peak detection, S-Peak detection, T-Peak detection, QRS complex detection,		SVM Training Data (75%) Testing Data (25%)	94.16%

** Critical Beat 1: Arrhythmia with high-speed frequency signal with short-term ECG signal, Critical Beat 2: Arrhythmia with high-speed frequency signal with short-term ECG signal, RBBB: Right Bundle Branch Block; LBBB: Left Bundle Branch Block*

We have acquired data from this machine for feature extractions and classifications by SVM, CNN, and RNN, such as ECG signal, heart rate, oxygen saturation, and respiration rate. The results show 95.62% accuracy by RNN, 96.56% by CNN, and 94.16% by SVM. We attempted a few different approaches to obtaining information on ECG beats. We believe that this device will meet the need for an urgent and reliable solution for remote monitoring of ECG signals and will help diagnose patients with cardiac abnormalities and assist cardiologists in analyzing patients' heart conditions via dynamic monitoring in a real-world application.

Acknowledgment

The authors wish to thank the Dept. of Biomedical Engineering and Dept. of Electronics and Communication Engineering staff and all professors for supporting equipment and other facilities.

Conflict of Interest & Fund

The authors declare that they have no Conflict of Interest. This work was not supported in part by a grant.

References

[1] P. K. Jain, A. K.P. K. Jain, A. K. Tiwari, "Heart monitoring systems—A review", *Computers in Biology and Medicine,* Volume 54,2014, Pages 1-13. https://doi.org/10.1016/j.compbiomed.2014.08.014.

[2] A. Gacek, "*An Introduction to ECG Signal Processing and Analysis*", In: Gacek, A., Pedrycz, W. (eds), ECG Signal Processing, Classification and Interpretation, pp. 21-46, 2011. https://doi.org/10.1007/978-0-85729-868-3_2

[3] Z. Sankari, H. Adeli, "HeartSaver: a mobile cardiac monitoring system for auto-detection of atrial fibrillation, myocardial infarction, and atrioventricular block," *Computers in biology and medicine* vol. Vol. 41, no. 4, pp. 211-214, 2011. https://doi.org/10.1016/j.compbiomed.2011.02.002

[4] N. Stojanovic, Y. Xu, A. Stojadinovic, L. Stojanovic, "Using Mobile-based Complex Event Processing to realise Collaborative Remote Person Monitoring. DEBS '14," *8th ACM International Conference on Distributed Event-Based Systems.* 2014, page 225. https://doi.org/10.1145/2611286.2611306

[5] M. A. Mahamdy, H. B. Riley, "Performance Study of Different Denoising Methods for ECG Signals," *Procedia Computer Science,* Volume 37, 2014, Pages 325-332. https://doi.org/10.1016/j.procs.2014.08.04800

[6] L. R. Yeh, W.C. Chen,H. Y. Chan,N. H. Lu, C. Y. Wang, W. C. Du, Y. H. Huang, S. Y. Hsu,T. B. Chen, "Integrating ECG Monitoring and Classification via IoT and Deep Neural Networks," *Biosensors (Basel).* 2021 Jun 8;11(6):188. doi: 10.3390/bios11060188. PMID: 34201215; PMCID: PMC8226863

[7] J.J. Huang, B. Chen, B. Yao and W. He, "ECG Arrhythmia Classification Using STFT-Based Spectrogram and Convolutional Neural Network," in *IEEE Access*, vol. 7, pp. 92871-92880, 2019, doi: 10.1109/ACCESS.2019.2928017.

[8] L. Alzubaidi, J. Zhang, A. J. Humaidi et al., "Review of deep learning: concepts, CNN architectures, challenges, applications, future directions," *J. Big Data* **8**, 53 (2021).

[9] R. Thilagavathy, R. Srivatsan, S. Sreekarun, D. Sudeshna, P. L. Priya and B. Venkataramani, "Real-Time ECG Signal Feature Extraction and Classification using Support Vector Machine," *2020 International Conference on Contemporary Computing and Applications (IC3A),* 2020, pp. 44-48, doi: 10.1109/IC3A48958.2020.233266.

[10] Guijin Wang, Chenshuang Zhang, Yongpan Liu, Huazhong Yang, Dapeng Fu, Haiqing Wang, Ping Zhang, "A global and updatable ECG beat classification system based on recurrent neural networks and active learning," *Information Sciences,* Volume 501, pp. 523 - 542,2019. https://doi.org/10.1016/j.ins.2018.06.062.

[11] F. T. Johura, S. M. R. Islam, M. Maniruzzaman and M. Hasan, "ECG signal for artrial fibrillation detection," *2017 International Conference on Electrical, Computer and Communication Engineering (ECCE)*, 2017, pp. 928-934, doi: 10.1109/ECACE.2017.7913036.

[12] J. R. Mou, S. M. Rabiul Islam, X. Huang and K. L. Ou, "A new approach of noise elimination methodology for ECG signal," *2017 International Conference on Electrical, Computer and Communication Engineering (ECCE)*, pp. 921 - 927, 2017 doi: 10.1109/ECACE.2017.7913035.

[13] H. Khorrami and M. Moavenian, "A comparative study of DWT, CWT and DCT transformations in ECG arrhythmias classification," *Expert Systems with Applications*, vol. 37, no. 8, pp. 5751–5757, 2010. https://doi.org/10.1016/j.eswa.2010.02.033

[14] N. Tabassum, S. M. R. Islam, X. Huang, "Novel Multirate Digital Filter for EEG on FPGA", *2nd International Conference on Electrical &Electronic Engineering (ICEEE), RUET, Rajshahi, Bangladesh*, 19-21 December 2017. doi: 10.1109/CEEE.2017.8412848.

[15] Mishra et al., "ECG Data Analysis with Denoising Approach and Customized CNNs", *Sensors*, vol. 22, no. 5, p. 1928, 2022. https://doi.org/10.3390/s22051928

[16] E. D. Übeyli, "Adaptive neuro-fuzzy inference system for classification of ECG signals using Lyapunov exponents," *Computer Methods and Programs in Biomedicine*, Volume 93, Issue 3, 2009, pp. 313-321. https://doi.org/10.1016/j.cmpb.2008.10.012

[17] Tomasini, Marco, Simone Benatti, Bojan Milosevic, Elisabetta Farella, and Luca Benini. "Power line interference removal for high-quality continuous biosignal monitoring with low-power wearable devices." *IEEE Sensors, vol.* 16, no. 10, pp. 3887-3895, 2016.

[18] K. Tanji, M.A.G de Brito,M.G. Alves,R. C. Garcia, G.L. Chen, N. R. N. Ama, "Improved Noise Cancelling Algorithm for Electrocardiogram Based on Moving Average Adaptive Filter," *Electronics* vol. *10*, no. 19, pp. 1 - 18, 2021, . https://doi.org/10.3390/electronics1019236

[19] N. Wang and S. Sun, "Event-triggered sequential fusion filters based on estimators of observation noises for multi-sensor systems with correlated noises", *Digital Signal Processing*, vol. 111, p. 102960, 2021. https://doi.org/10.1016/j.dsp.2020.102960

[20] S. M. Anwar , M. Gul, M. Majid, M. Alnowami, "Arrhythmia Classification of ECG Signals Using Hybrid Features," *Comput Math Methods* Med. 2018 Nov 12;2018:1380348. doi: 10.1155/2018/1380348. PMID: 30538768; PMCID: PMC6260536.

[21] C. Jha and M. Kolekar, "Cardiac arrhythmia classification using tunable Q-wavelet transform based features and support vector machine classifier", *Biomedical Signal Processing and Control*, vol. 59, p. 101875, 2020. https://doi.org/10.1016/j.bspc.2020.101875

[22] A. Darmawahyuni et al., "Deep Learning with a Recurrent Network Structure in the Sequence Modeling of Imbalanced Data for ECG-Rhythm Classifier", *Algorithms*, vol. 12, no. 6, p. 118, 2019. https://doi.org/10.3390/a12060118

[23] Z. He, Y. Chen, D. Zhang, W. Yin, and H. R. Karimi. "A new intelligent ECG recognition approach based on CNN and

improved ALO-SVM." *Signal, Image and Video Processing* (2022): 1-8. https://doi.org/10.1007/s11760-022-02300-5

SHEIKH MD. RABIUL ISLAM received the B.Sc. In Engineering (ECE) Khulna University, Bangladesh, M.Sc. in Telecommunication Engineering from the University of Trento, Italy, in October, and Ph.D. from the University of Canberra, Australia, in 2015. He joined as a Lecturer in the Department of Electronics and Communication Engineering of Khulna University of Engineering & Technology, Khulna, in 2004, where he joined as an Assistant Professor in the same department in 2008. Also, he joined Associate Professor in 2015 and a Professor in 2018 in the same department.

He has been given six M.Sc. Engineering at Dept. of ECE and one M.Sc. Engineering (BME) at Dept. of Biomedical Engineering. He has also completed five projects by a funded university grant commission. He has published two book chapters, 35 journals, and 37 International conferences. His research interests include biomedical engineering and Public Health. Recently, Brain function on EOG, EEG, fMRI, and fNIRS, public health on research has been tackled. He is affiliated with an IEEE member. Further info on his homepage: https://www.kuet.ac.bd/ece/rabiul/

AKRAM HOSSAIN received his B.Sc. degree in Biomedical Engineering (BME) from Khulna University of Engineering & Technology (KUET), Khulna, Bangladesh, in 2022. His current research focuses on data science, machine learning, deep learning and neural network in the biomedical sector, and network security.

Asif Abdullah received his B.Sc. degree in Biomedical Engineering from Jashore University of Science and Technology, Jashore, 7408, Bangladesh, in 2020. His current research focuses on Biomedical Instrumentation, Biomedical Signal Processing, Biomaterials, and Bioinformatics.

Authors' contribution: Conceptualization S.M.R.I, Circuit Design S.M.R.I and A.H., Data Acquisition and Real-Time Visualization A.H., Classification A.A., Manuscript Writing A.H., And A.A., Review and Editing S.M.R.I, A.A. and A.H. All authors read and approved the final revision of the manuscript.

JENRS

Received: 07 October 2022, Revised: 10 November 2022, Accepted: 11 November 2022, Online: 30 November 2022

DOI: https://dx.doi.org/10.55708/js0111003

Enhancing the Contribution of Recycled Asphalt Shingles to Asphalt Binders Using Rejuvenators

Eslam Deef-Allah*, Magdy Abdelrahman

Department of Civil, Architectural and Environmental Engineering, Missouri University of Science and Technology, Rolla, MO 65409, USA
*Corresponding author: Eslam Deef-Allah, Tel: 5735786643, Email: emddkc@mst.edu

ABSTRACT: Recycled asphalt shingles (RAS) have been a valuable recycled component in asphalt mixes for decades. However, research into how the aged and oxidized air-blown RAS binder interacts with the neat asphalt binders in asphalt mixtures is underway. Furthermore, due to the stiffness of RAS binders, RAS-containing asphalt mixtures are prone to significant cracking, particularly at low temperatures. As a result, an innovative technique was developed and used in this study to increase the contribution of RAS particles in the asphalt binder. This technique was primarily dependent on interacting RAS particles with rejuvenators before mixing them with the asphalt binder. Moreover, this technique allowed the oxidized and aged binders in the RAS to absorb aromatics to compensate for the lost low-molecular-weight fractions during the air-blowing process and alter their aged behavior. Five rejuvenators were utilized, including four pyrolysis oils (B2A, P4, P8, and P4D) and one recycling agent (Evoflex). One source of post-consumer RAS was collected, milled, and sieved into two sizes. The rejuvenator was chosen to weigh 45% of the RAS, except for the P4D, which contained a double amount of P4 oil and weighed 90% of the RAS. RAS or the RAS that interacted with oils, was mixed with one source of asphalt binder with a performance grade of 76–16. The RAS with rejuvenator samples weighing 7.5% and 15% of the asphalt binder interacted with the neat binder. The addition of P4D or Evoflex to RAS reduced the stiffness and elasticity of the modified asphalt binders due to the RAS particles' absorption of aromatics in oils. This trend improved the modified binders' fatigue and thermal cracking resistance. Milled RAS particles of a smaller size (50-100) reacted with oils more than RAS particles of a bigger size (30-50), which caused stiffer properties for the binders modified with the smaller RAS particle size.

KEYWORDS: Recycled Asphalt Shingles, Rejuvenators, Pyrolysis Oil, Milling

1. Introduction

The usage of recycled asphalt shingles (RAS) in the pavement industry is growing due to the valuable constituents that make them more suitable for use with asphaltic mixes [1]. RAS contains oxidized air-blown asphalt binders, polymers, granules, mineral fillers, and fibers [2–4]. Utilizing RAS in asphalt mixes modifies the performance of the total binders in these mixes due to interactions between RAS and the virgin binders [4–6]. In asphalt mixtures, two types of shingles are permitted: Manufactured waste and tear-off (post-consumer) shingles [7, 8]. Manufactured waste shingles are waste products of the shingle manufacturing process, whereas post-consumer shingles are shingles that primarily originate from residential and commercial building roofs after their useful lives have ended [9]. When compared to the binders incorporated in the manufactured waste shingles, the oxidation impact on the post-consumer shingles created stiffer characteristics for their asphalt binders [10, 11].

The use of RAS in asphalt mixes minimizes the demand for natural resources, emissions during the manufacturing process, and the amount of material discarded in landfills [12, 13]. The asphalt binders in RAS are more difficult to interact with virgin asphalt binder in asphalt mixes than asphalt binders in reclaimed asphalt pavement (RAP) [5, 14–16]. Because the oxidized and aged binders in RAS enhanced the stiffness and elasticities of the binder, utilizing RAS in asphalt mixes increased the rutting resistance of the mixes and extracted asphalt

binders as compared to virgin mixes and binders [4, 5]. However, increasing the stiffness of the asphalt binder lessened its ductility, and relaxation potential, and increased its cracking capability [6, 17, 18].

The wet process of adding RAS to asphalt binders boosted fatigue cracking resistance, resulting in higher fatigue life values. However, the Superpave fatigue parameter (G*.sinδ) values increased, suggesting decreased fatigue cracking resistance [19]. Another study revealed that using the RAS binder with a neat binder did not influence G*.sinδ values when compared to the neat binder value [20]. Using RAS in asphalt mixes enhanced the fatigue cracking resistance of the extracted binders when compared to extracted binders from mixtures containing binders with the same performance grade (PG) but lower RAP percentages [21, 22]. This was due to the polymeric components included in shingles [5] that enhance the fatigue cracking resistance. Using RAS as a modifier with the neat binder influences the low-temperature performance of the modified asphalt binder [6,23]. When the RAS binder was blended with neat binder, the low temperature increased by 0.4°C for every 1% of asphalt binder replaced by RAS [23]. When compared to binders extracted from RAP-containing mixes, the use of RAS exacerbated the low-temperature characteristics of extracted binders [6].

Using rejuvenators balances the performance of the modified asphalt binders by marginally decreasing the binders' stiffness at high temperatures and increasing their fluidity at intermediate and low temperatures [24–26]. They vary from organic oils (such as vegetable oil and tall oil) to petroleum-based rejuvenators (such as used motor oil and aromatic extracts) [27]. Evoflex as a rejuvenator or recycling agent enhanced the contribution of the aged binders in recycled components in asphalt mixes by enhancing the mobility of these aged binders [5, 14]. Because pyrolysis oil has a high concentration of aromatics [28, 29], it was used as a rejuvenating agent, allowing the aged binders to achieve characteristics equivalent to the unaged asphalt binder [30]. Pyrolysis oil is produced by the thermal decomposition of tires in an oxygen-deficient environment, which also produces fumes and solid residue [31]. It was assumed that it would interact with RAS to adjust its aged binder with low-molecular-weight fractions before being introduced to the asphalt binder.

An innovative methodology was adopted in this study to enhance the role of RAS in asphalt binders. First and foremost, RAS particles were milled to improve their compatibility with the rejuvenators before being introduced to the asphalt binder. Then, the milled RAS particles were interacted with rejuvenators and preheated in the oven before mixing with asphalt binders to alleviate the issues associated with employing RAS in asphalt mixes at low temperatures. This technique enables the oxidized and aged binders in RAS to absorb aromatics to compensate for the lost low-molecular-weight fractions during the air-blowing process and adjust their aged behavior. The key to this novel approach was the creation of a homogenous modified asphalt binder blend with superior performance at high, intermediate, and low temperatures.

2. Materials and Methods

2.1. Materials

One source of asphalt binder was used with a PG of 76–16, and one source of post-consumer RAS was selected. The RAS particles were cleaned from the wood and plastic pieces, then they were milled using a vibratory disc mill. The particles of RAS were milled to enhance their compatibility with the rejuvenators and asphalt binder using the wet process. The milled particles were sieved on #30, #50, #100, #200, and a pan. Two particle sizes of RAS were utilized: The first size was 30-50 and the second size was 50-100. The first particle size represents particles passed from #30 and retained on #50, and the second particle size simulates particles passed from #50 and retained on #100. Different types of rejuvenators were used, which represented pyrolysis oils (B2A, P4, P8, and P4D) and a recycling agent (Evoflex). These rejuvenators were introduced to the RAS to decrease the stiffness of the binder in the RAS by absorbing aromatics from the rejuvenators, and then the blend of RAS plus rejuvenator was mixed with the neat asphalt binder. More details about the used rejuvenators are introduced in Table 1.

Table 1: Details of Rejuvenators

Rejuvenator Code	Details of the As-Received Rejuvenators
B2A	Tire oil was collected from trays 3 and 4 and post-cooked at 510° to 868°F
P4	Tire oil was collected from combined trays and post-cooked at 570°F for 4 hrs
P8	Tire oil was collected from combined trays and post-cooked at 570°F for 8 hrs
P4D	Double the percentage of P4 oil
E	Evoflex CA-9

2.2. RAS, Asphalt Binder, and Rejuvenators Interactions

Milled RAS with two particle sizes (Figures 1-a and 1-b) has interacted with the different types of rejuvenators as indicated in Figures 1-c and 1-d. The weight of the rejuvenator was selected to be 45% by the weight of the RAS except for the P4D—a double percentage of P4 oil—the weight of the P4 oil was 90% by the weight of the RAS. After stirring the rejuvenator with RAS manually, the interacted RAS with rejuvenator samples were transferred to the oven at 90°C and kept there for 6 hrs to enhance the absorbance of RAS to aromatics. Finally, the RAS with rejuvenator samples (Figures 1-e and 1-f)—with a weight of 7.5% and 15% by the weight of the asphalt binder—

interacted with the PG 76–16 asphalt binder using a high shear mixer at 190°C interaction temperature, 1800-rpm interaction speed, and 4-hrs interaction time. Modified binder samples were collected at 0.5-, 1-, 2-, and 4-hrs interaction times during the interaction process for further analyses.

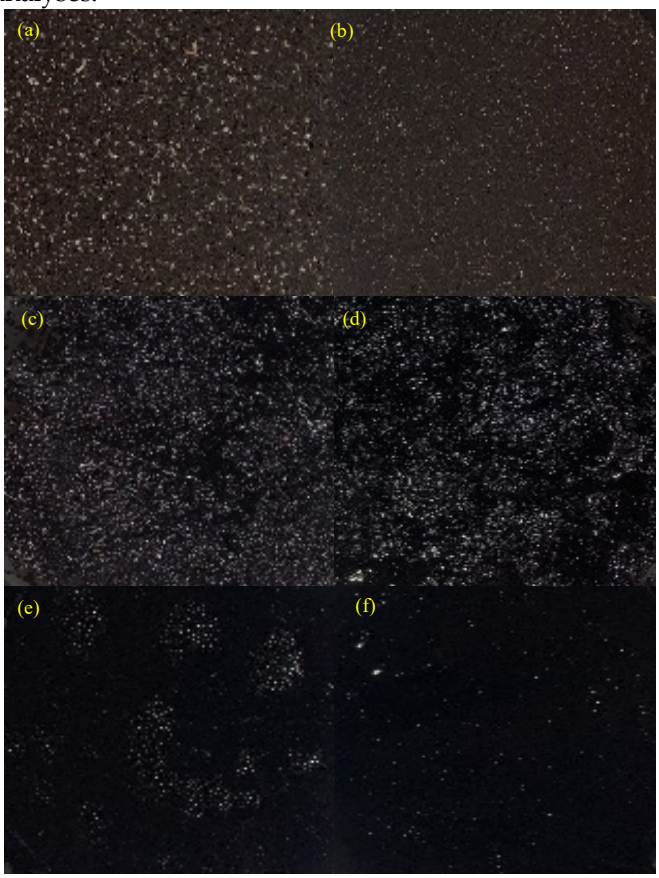

Figure 1: Milled RAS with a Size of (a) 30-50 and (b) 50-100, Milled (c) 30-50 and (d) 50-100 RAS and Rejuvenator before Heating, and Milled (e) 30-50 and (f) 50-100 RAS and Rejuvenator after Heating

2.3. Methods

The steps followed to achieve the experimental design of this study are depicted in Figure 2. Four major steps were followed. The RAS particles were milled in the first step. The second step aimed to interact rejuvenators with RAS particles. In the third step, RAS and interacted RAS with the rejuvenators were mixed with the neat binder. The fourth step included the characterization of the neat and modified asphalt binders. The following subsections explain the full experimental testing that was conducted in detail.

2.3.1. Short-Term Aging for Asphalt Binders

Short-term aging was carried out using the rolling thin film oven (RTFO) device according to ASTM D2872-19 [32] for neat and modified asphalt binders. The mass loss percentage was calculated for the neat and modified asphalt binders after the RTFO test.

2.3.2. Long-Term Aging for Asphalt Binders

Long-term aging was carried out according to ASTM D6521-19a [33] using a pressure aging vessel (PAV) for the neat and modified asphalt binders.

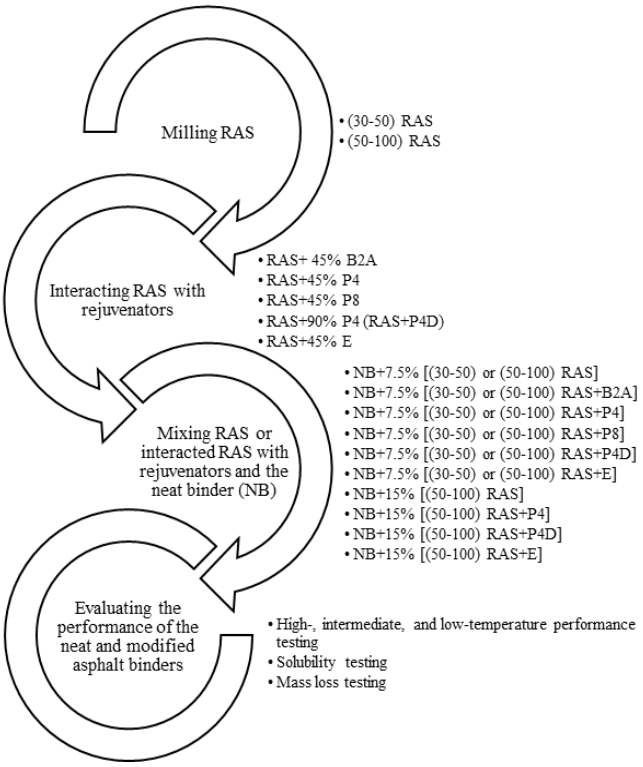

Figure 2: Experimental Design

2.3.3. High- and Intermediate-Temperature Rheological Properties of Asphalt Binders

A Dynamic Shear Rheometer (DSR) was used following ASTM D7175-15 [34] to characterize the neat and modified asphalt binders' high- and intermediate-temperature properties. Specimens with a thickness of 1 mm and 25 mm diameter for the original and RTFO-aged binders were tested. Additionally, 2 mm-thick and 8 mm-diameter specimens were used for PAV binders.

The temperature sweep test was implemented for the original, RTFO-aged, and PAV-aged asphalt binders at different temperatures. For the original and RTFO-aged binders, 70°C, 76°C, and 82°C temperatures were selected. For the PAV-aged binders, 28°C, 31°C, and 34°C temperatures were selected. For the frequency sweep testing, conducted on the original binders, three temperatures were selected (70°C, 76°C, and 82°C) through different frequencies (50 rad/s to 0.5 rad/s). The master curves were analyzed, using the frequency sweep test results, at 76°C as a reference temperature.

A multiple stress creep recovery (MSCR) test was conducted following ASTM D7405-20 [35] to evaluate the resistance of RTFO binders to rutting distress. This was achieved by calculating the percentage of recovery (%R) and non-recoverable creep compliance (J_{nr}) at 76°C by applying ten creep cycles at two different levels of stress (0.1 kPa and 3.2 kPa). For each creep cycle, the loading time was 1 sec, and the unloading time (recovery) was 9 sec. The %R reflected the binders' elasticities, and the J_{nr} indicated the binders' stiffnesses.

2.3.4. Low-Temperature Rheological Properties of Asphalt Binders

Low-temperature properties of neat and modified asphalt binders were evaluated according to ASTM D6648-08 [36] using a bending beam rheometer (BBR).

2.3.5. Insoluble Percentages of Asphalt Binders

Because of the use of RAS in the modified asphalt binders, the solubility of the asphalt binders in toluene was evaluated following ASTM D2042-22 [37].

3. Results and Discussion

3.1. Mass Loss Results

The mass losses after the RTFO test were calculated and depicted in Figure 3 for the neat and modified asphalt binders at 2- and 4-hrs interaction times. The percentages of mass losses were under the maximum threshold (1%) except for the binder modified by 15% RAS plus P4D and interacted at 2 hrs. The use of RAS with the neat binder decreased the percentage of mass loss when compared to the percentage of the neat binder. The lowest percentage of mass loss was recorded for the neat binder modified by 7.5% RAS. For asphalt binders modified by RAS and rejuvenators, the percentages of mass losses increased due to the existence of low-molecular-weight fractions (aromatics) in the rejuvenators that were lost after the RTFO process. Furthermore, increasing the interaction time from 2 hrs to 4 hrs decreased the percentage of mass losses due to the evaporation of the aromatics during the interaction processes. The mass loss percentages for the modified binders with RAS (30-50) were higher than those of the modified binders with RAS (50-100). This occurred because the particles of RAS with a size of 50-100 absorbed more oil and had more compatibility with the binder than the particles of RAS with a size of 30-50. For the 50-100 RAS, increasing the percentage of the interacted RAS with oils from 7.5% to 15% by the weight of the neat binder caused an increase in the mass loss percentages. This happened due to the higher amount of aromatics that were lost from the binders modified with higher percentages of the interacted RAS with oils.

3.2. High-Temperature Rheological Results

The MSCR test results (%R and J_{nr}) are presented in Figure 4 for the RTFO neat and modified asphalt binders interacted at 4 hrs. The %R results at 0.1 and 3.2 kPa stress levels and 76°C are depicted in Figure 4-a, and the J_{nr} results at 0.1 and 3.2 kPa stress levels and 76°C are introduced in Figure 4-b. The general trend was that the %R values for the modified binders were higher than that of the neat binder due to the existence of the oxidized air-blown RAS binder that increased the elasticity (%R). The highest %R values were noted for the neat binder modified by RAS+B2A, and the lowest %R values were for the neat binder modified by RAS+E. The stiffness values of the modified binders were higher than for the neat binder by showing lower J_{nr} values except for samples modified by RAS (30-50) and P4D oil and for the samples modified by RAS+E. The lowest J_{nr} values were noted for the neat binder modified by RAS+B2A, and the highest J_{nr} values were for the neat binder modified by RAS+E.

When comparing binders modified by the RAS+P4 and the RAS+P8, the binders modified by the RAS+P4 had lower stiffness and elasticity values than those of the binders modified by the RAS+P8. Furthermore, the binders modified by the RAS+P4D oil had lower stiffness and elasticity values than those of the modified binders by RAS+P4.

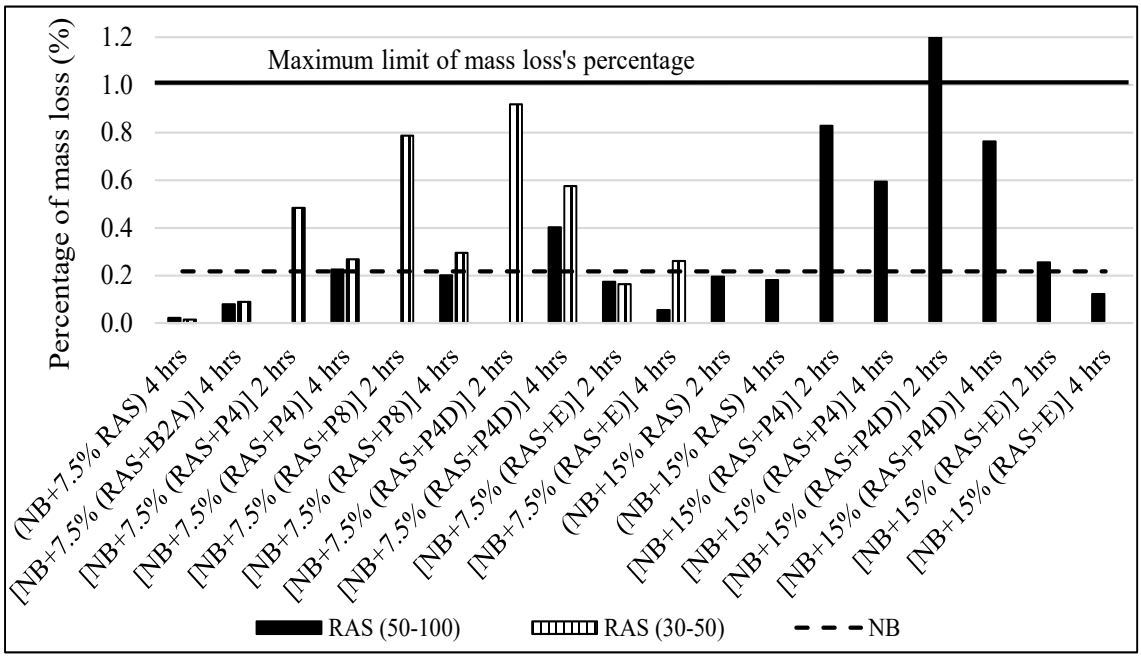

Figure 3: Mass Losses for Neat and Modified Binders

When comparing the RAS particles of two sizes, the general trend was that the RAS particles with the smaller size showed higher elasticities (higher %R values) and higher stiffnesses (lower J_{nr} values). More compatibility happened between the RAS particles with a smaller size and the asphalt binder than between particles with a larger size and the same binder. These results confirmed that binders modified by RAS and B2A oil had the highest stiffnesses and elasticities, while binders modified by RAS and E oil showed the lowest stiffnesses and elasticities. Increasing the percentage of RAS from 7.5% to 15% by the weight of the neat binder showed an increase in stiffness and elasticity due to the oxidized air-blown binder in the RAS. However, increasing the percentage of the interacted RAS with oils from 7.5% to 15 % by the weight of the neat binder depicted a decrease in elasticity and stiffness. This reflected that interacting RAS with rejuvenators decreases the stiffness of the oxidized air-blown binder in RAS by absorbing aromatics from rejuvenators.

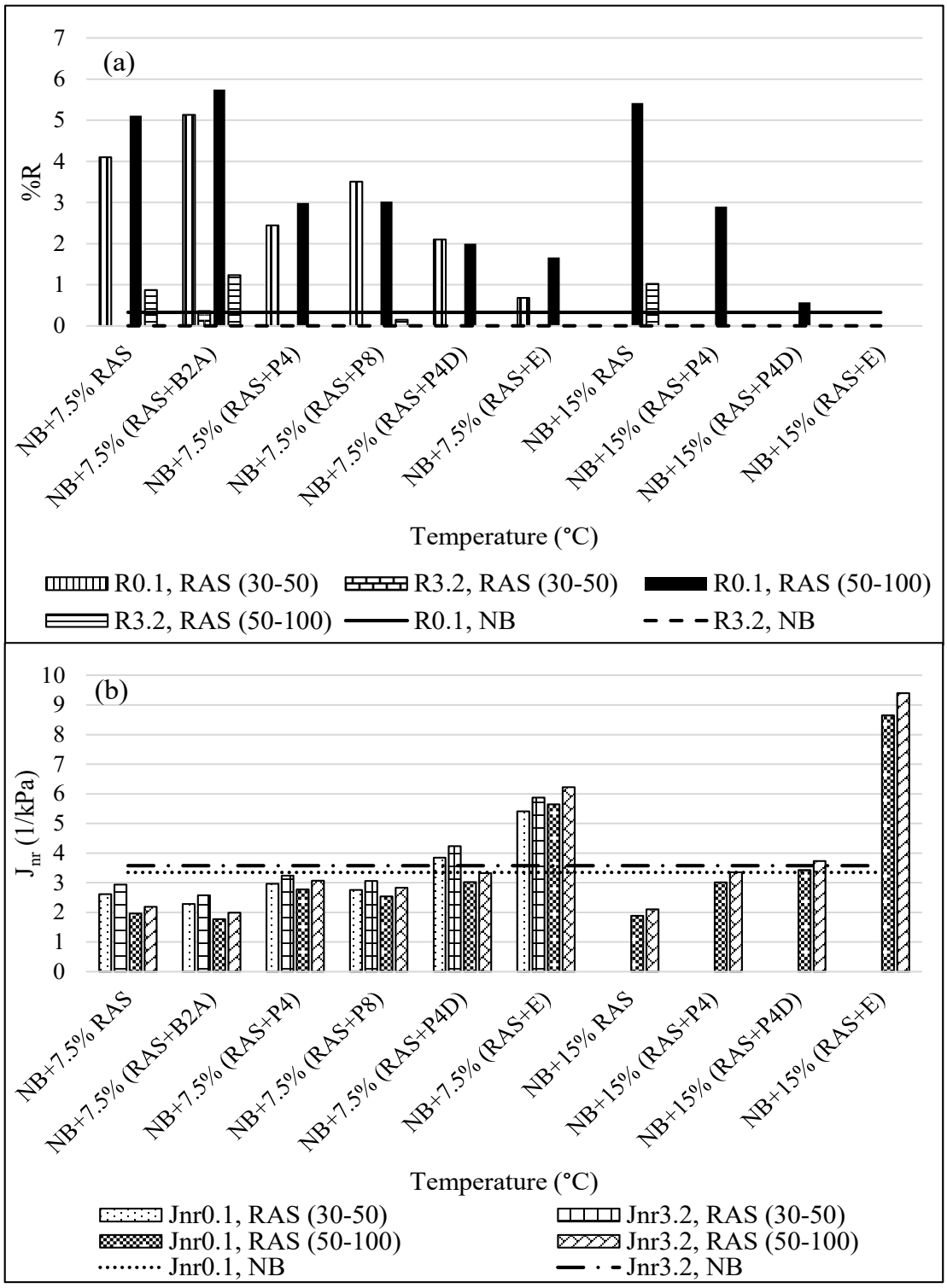

Figure 4: MSCR Results: (a) %R and (b) J_{nr} Measured at 76°C for the RTFO Neat and Modified Binders Interacted at 4 hrs

The rutting parameter (G*/sinδ) values obtained from the temperature sweep test results are represented in Figures 5 and 6 for the original neat and modified asphalt binders by 7.5% RAS or 7.5% RAS plus rejuvenators at different temperatures. Increasing the interaction time increased the G*/sinδ values of the modified binders because more compatibility took place between the RAS binder and neat binder, and more aromatics were lost from the rejuvenators. The modified binders with RAS (Figure 5-a) showed higher G*/sinδ values at different temperatures than that obtained for the neat binder because of the oxidized air-blown binder included in the RAS. Adding E and P4D oils to RAS counteracted the effect of the oxidized air-blown binder in the RAS by decreasing the stiffness of the modified asphalt binders (note Figures 6-b and 6-c). When comparing the modified binders with RAS+B2A, RAS+P4, and RAS+P8 in Figures 5-b, 5-c, and 6-a, the binder modified with RAS+P4 was the best choice because it has the lowest stiffness. As discussed earlier, the smallest RAS size (50-100) interacted more with the rejuvenators, causing more compatibility with the neat binder, than the largest size of RAS (30-50). That's why modified binders with the RAS (50-100) showed more stiffnesses than the binders that interacted with the RAS (30-50). These results are confirmed with the temperature sweep test results presented in Figure 7 for the neat binder and modified binders by 7.5% RAS or 7.5% RAS plus rejuvenators and interacted at 0.5-hr and 4-hrs interaction times. Furthermore, increasing the interaction time from 0.5 hr in Figure 7-a to 4 hrs in Figure 7-b caused more compatibility between the neat binder and the RAS binder.

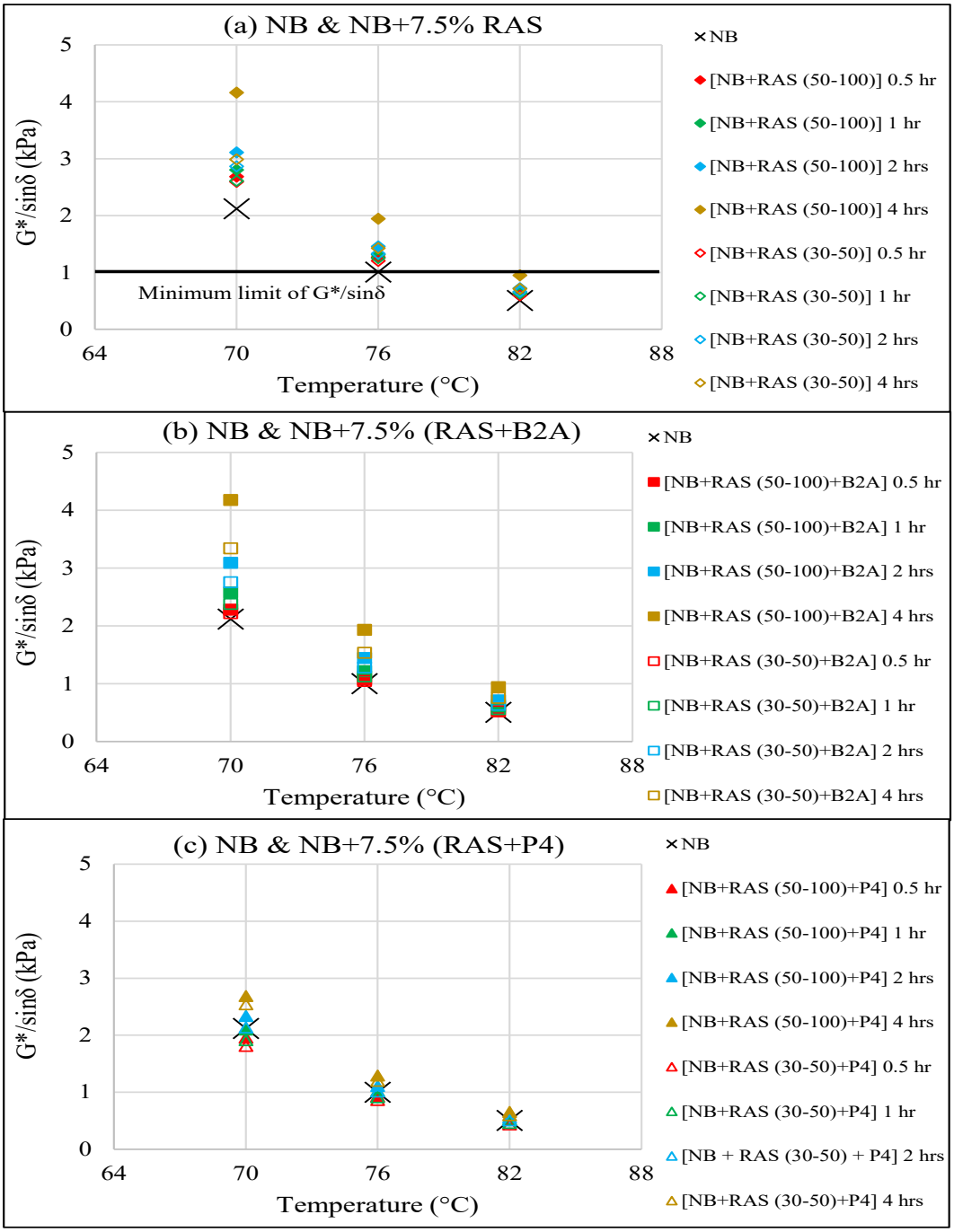

Figure 5: Temperature Sweep Results for the Original Neat and Modified Binders with (a) 7.5% RAS, (b) 7.5% RAS+B2A, and 7.5% RAS+P4

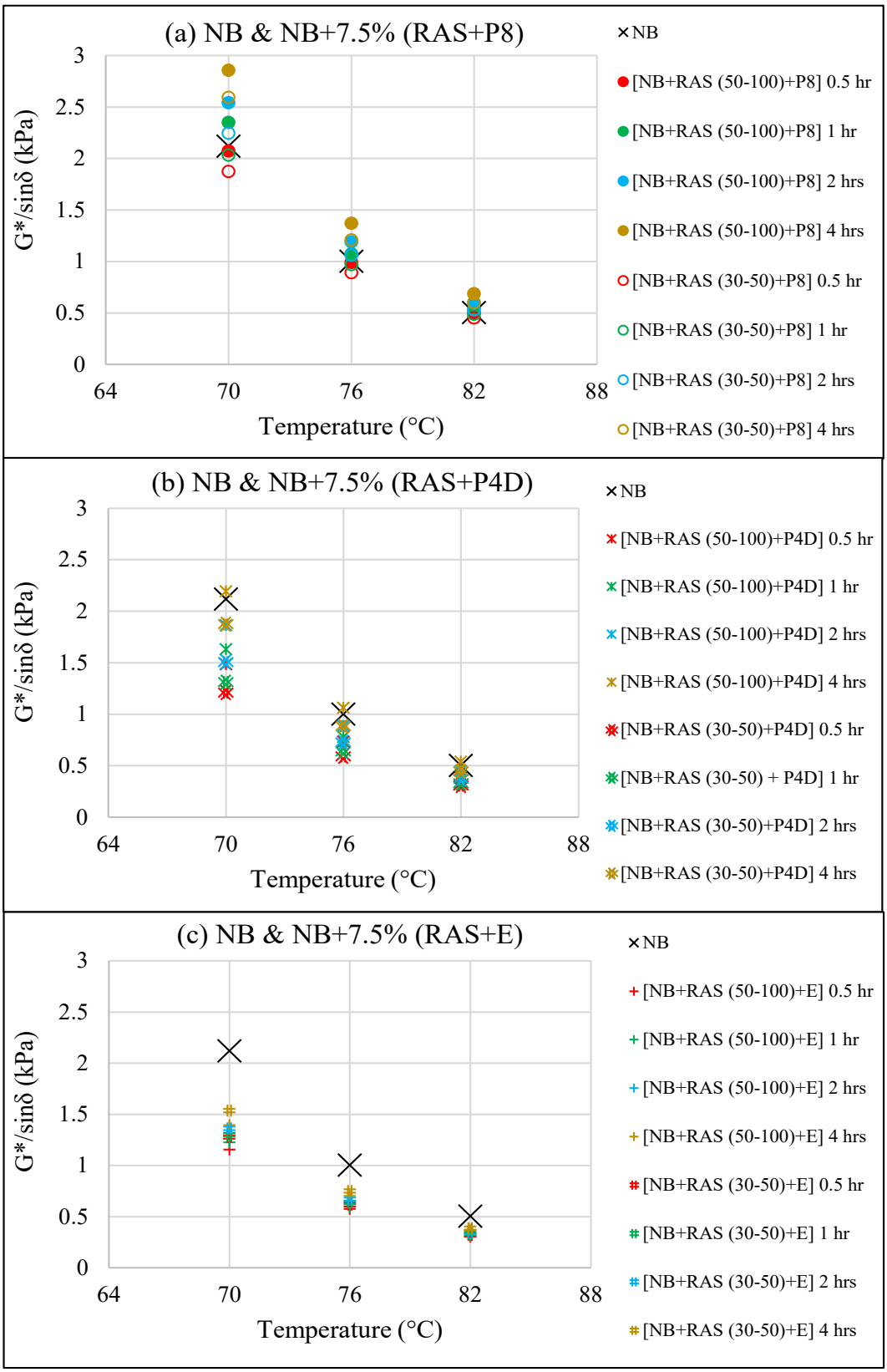

Figure 6: Temperature Sweep Results for the Original Neat and Modified Binders with (a) 7.5% RAS+P8, (b) 7.5% RAS+P4D, and (c) 7.5% RAS+E

The effect of increasing the percentage of RAS or the interacted RAS with oils was explored in Figure 8. Doubling the percentage of RAS in asphalt binders increased the G*/sinδ values of the modified asphalt binders until 2-hrs interaction time (note Figure 8-a). At 4-hrs interaction time, the modified asphalt binder with 7.5% RAS showed higher G*/sinδ values than the modified asphalt binders with 15% RAS. This revealed that more interactions occurred between RAS and the neat binder at the 4-hrs interaction time for the sample modified by 7.5% RAS. This agrees with the results discussed in Figure 3: The modified binder with a 7.5% RAS had a lower mass loss percentage than the modified binder with a 15% RAS. For modified asphalt binders with RAS+P4, RAS+P4D, and RAS+E, increasing the percentage of the interacted RAS with oils from 7.5% to 15% showed a reduction in the G*/sinδ values because more aromatics were absorbed by the RAS particles.

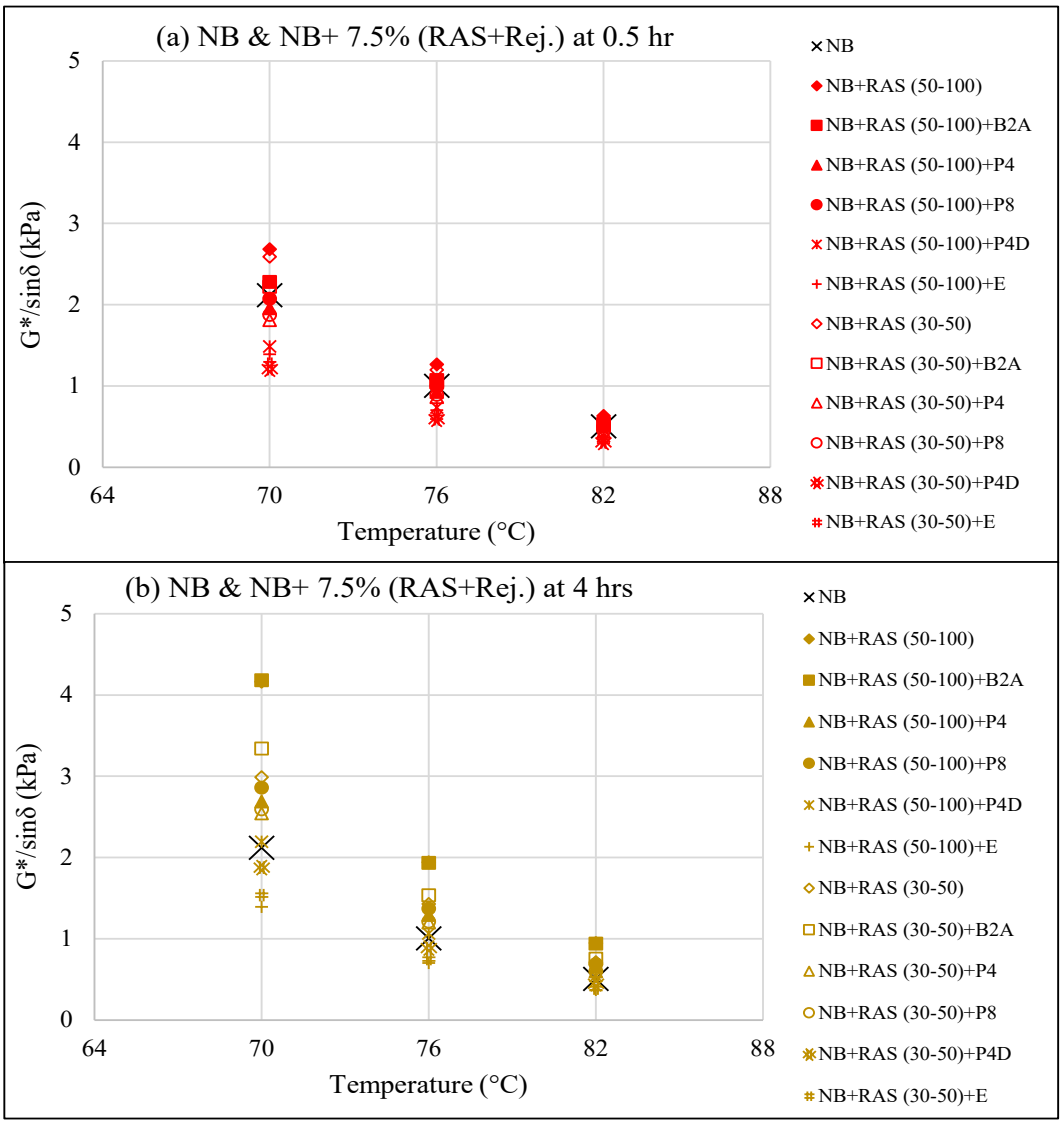

Figure 7: Temperature Sweep Results for the Original Neat and Modified Binders by 7.5% RAS Plus Rejuvenators at (a) 0.5-hr and (b) 4-hrs Interaction Times

The master curves for the original neat and modified asphalt binders are presented in Figures 9 to 10. Two parameters were illustrated and measured at 76°C in these figures: The complex shear modulus (G*) and phase angle (δ). The modified asphalt binders with RAS (50-100) showed higher stiffnesses (higher G*) and higher elasticities (lower δ) than the asphalt binders modified with RAS (30-50), especially at the 4-hrs interaction time (Figure 10). Increasing the interaction time caused more stiffnesses and elasticities for the modified asphalt binders for two reasons: The first reason was the more interactions between the RAS and asphalt binders, and the second was due to the loss of aromatics included in the modified binders.

Generally, using RAS to modify the neat binder caused higher stiffness and elasticity values when compared to the neat binder values. Adding rejuvenators to the RAS decreased the stiffnesses and elasticities of the modified binders because of the effect of the low-molecular-weight fractions (aromatics) in the rejuvenators. When the B2A oil was added to the RAS, it did not introduce a superior enhancement in the G* and δ values for the modified binders when compared to the values of the binders modified by the RAS only. However, the use of P4 and P8 oils with RAS to modify asphalt binder showed a better enhancement in the G* and δ values, presenting lower G* and higher δ values than the values of the asphalt binders modified by RAS only. The best enhancement in the G* and δ values were obtained by interacting the RAS with P4D or E oil: The lowest G* and the highest δ values were obtained for modified asphalt binders by RAS+E or RAS+P4D.

Increasing the RAS percentage from 7.5% to 15% caused an increase in the stiffness and elasticity values of the modified asphalt binder at a 0.5-hr interaction time due to the aged binder in the RAS. However, for RAS-modified binders that interacted at a 4-hrs interaction time, a binder with a lower RAS percentage (7.5%) had the highest stiffness and elasticity values than a binder with a higher RAS percentage (15%). This occurred because more interactions happened between RAS with a lower percentage and neat binder than between neat binder and a higher RAS percentage.

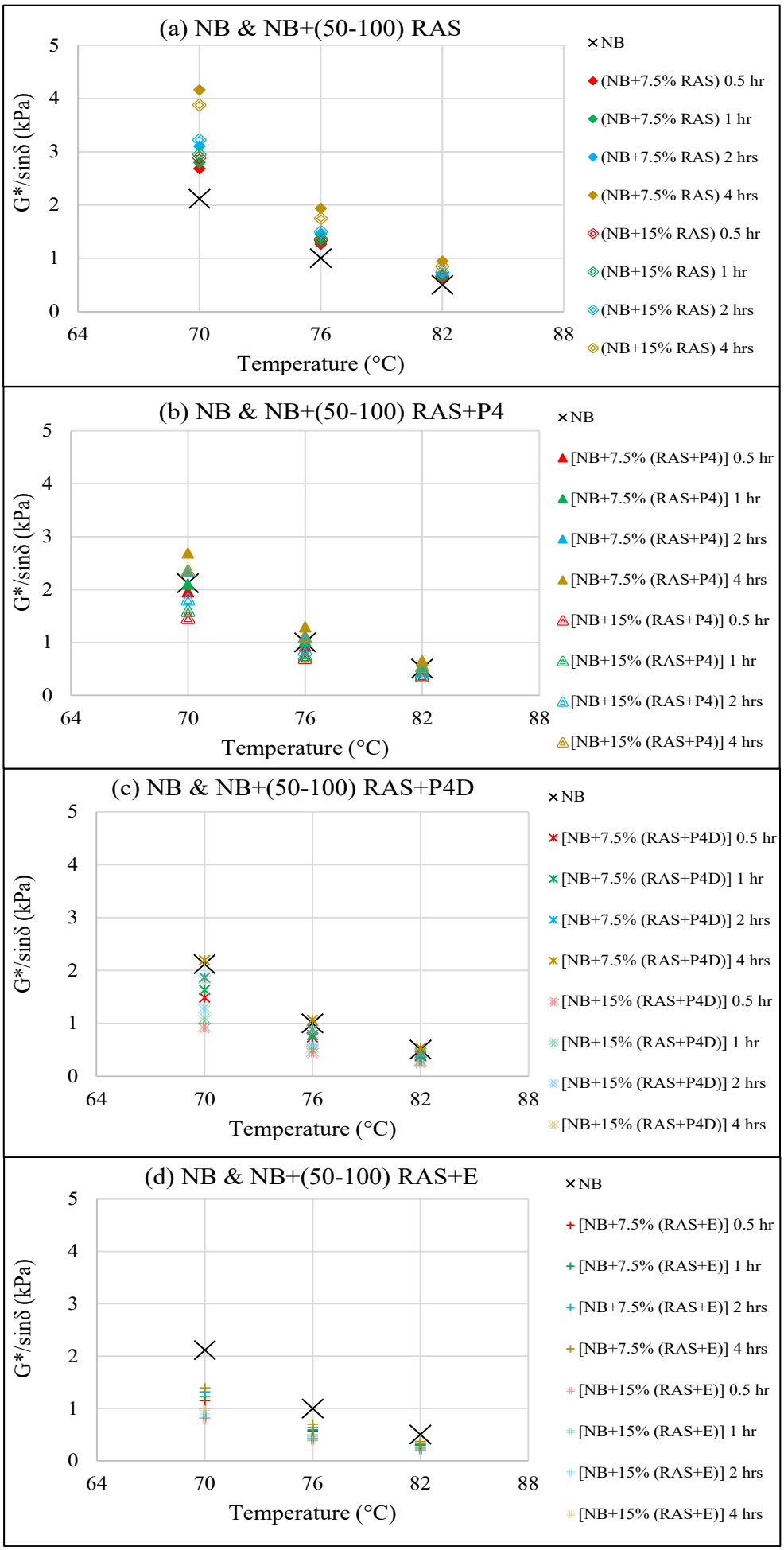

Figure 8: Temperature Sweep Results for the Original Neat and Modified Binders by (a) 50-100 RAS, (b) 50-100 RAS+P4, (c) 50-100 RAS+P4D, and (d) 50-100 RAS+E

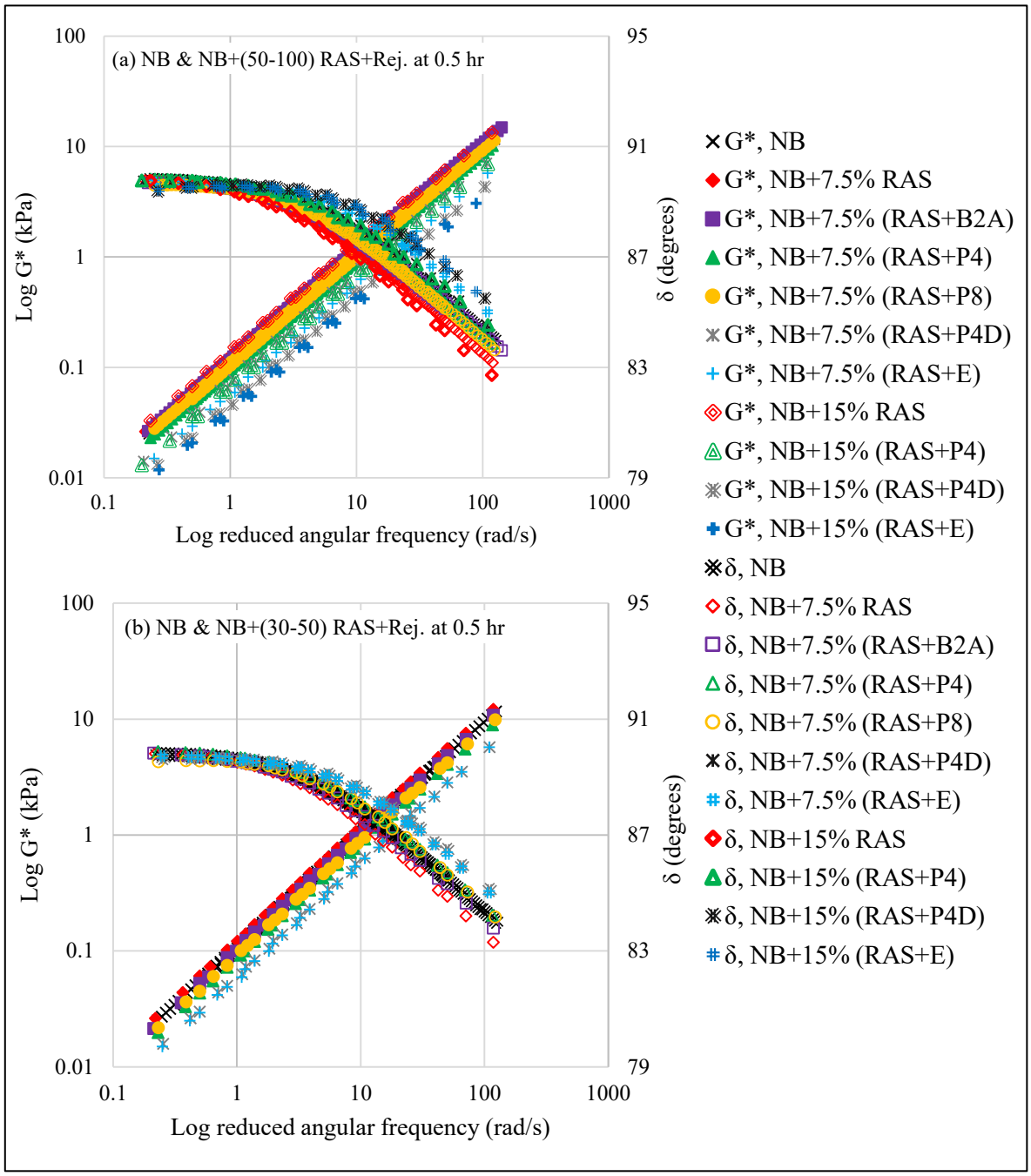

Figure 9: Master Curves for the Original Neat and Modified Binders with (a) 50-100 RAS Plus Rejuvenators and (b) 30-50 RAS Plus Rejuvenators Interacted at 0.5 hr

The temperature sweep test results for the RTFO neat and modified asphalt binders interacted at 4 hrs are displayed in Figure 11. The highest stiffnesses were for the modified asphalt binders with RAS+B2A and followed by the binders modified by RAS only. The lowest stiffness values were for the binder modified by RAS+E and followed by the binder modified by RAS+P4D. Furthermore, the general trend of most of the modified samples is that using RAS particles with smaller sizes caused more compatibility with the rejuvenators and neat binder than the RAS particles with larger sizes. That's why the modified asphalt binders with the interacted (50-100) RAS had higher resistance to rutting than the resistance of the modified binders with the interacted (30-50) RAS. Using E oil with two sizes of RAS and P4D oil with a RAS size of 30-50 to modify the neat binder led to stiffnesses lower than the values of the neat binder. From Figure 11-b, increasing the RAS percentage from 7.5% to 15% caused higher stiffness values for the modified asphalt binders. More interactions happened between RAS and neat binder during the RTFO process, which revealed higher G*/sinδ values for the modified binder with the higher RAS content (15%). However, increasing the percentage of RAS that interacted with oils showed a reduction in the G*/sinδ values due to the softness effect of the absorbed oil by RAS.

3.3. Intermediate-Temperature Rheological Results

The temperature sweep test results for the PAV neat and modified asphalt binders interacted at 4 hrs are shown in Figure 12. Using RAS with a size of 50-100 to modify the neat binder caused a deterioration in the fatigue resistance

when compared to the neat binder by showing higher G*.sinδ values. However, using the same source of RAS with a larger size (30-50) showed better resistance to fatigue cracking than the neat binder. The best enhancement in fatigue cracking resistance was for the neat binders modified by RAS and E oil. Increasing the RAS or the interacted RAS with oils percentages in the modified asphalt binder showed higher resistance to fatigue cracking because of the effect of RAS and oils to decrease the G*.sinδ values.

3.4. Low-Temperature Rheological Results

The low-temperature rheological properties at −16°C and −20°C of the PAV neat and modified asphalt binders interacted at 4 hrs are deemed in Figure 13. Using RAS with the neat binder did not significantly alter the low-temperature rheological properties of the modified asphalt binder. However, the use of RAS+B2A increased the stiffness values of the modified asphalt binder (Figure 13-a). The use of RAS+P4 and RAS+P4D decreased the stiffness of the modified asphalt binders. The best enhancement in the low-temperature rheological properties of the binders was obtained for the samples modified by RAS+E: These samples had the lowest stiffness values and the highest m-values. No specific trend could be observed when comparing the stiffness and m-value results of the modified binders by rejuvenators and two particle sizes of RAS. Increasing the RAS or the interacted RAS with oils in the modified binders enhanced the resistance to low-temperature cracking by showing higher m-values and lower stiffness values, which agrees with the intermediate-temperature cracking results.

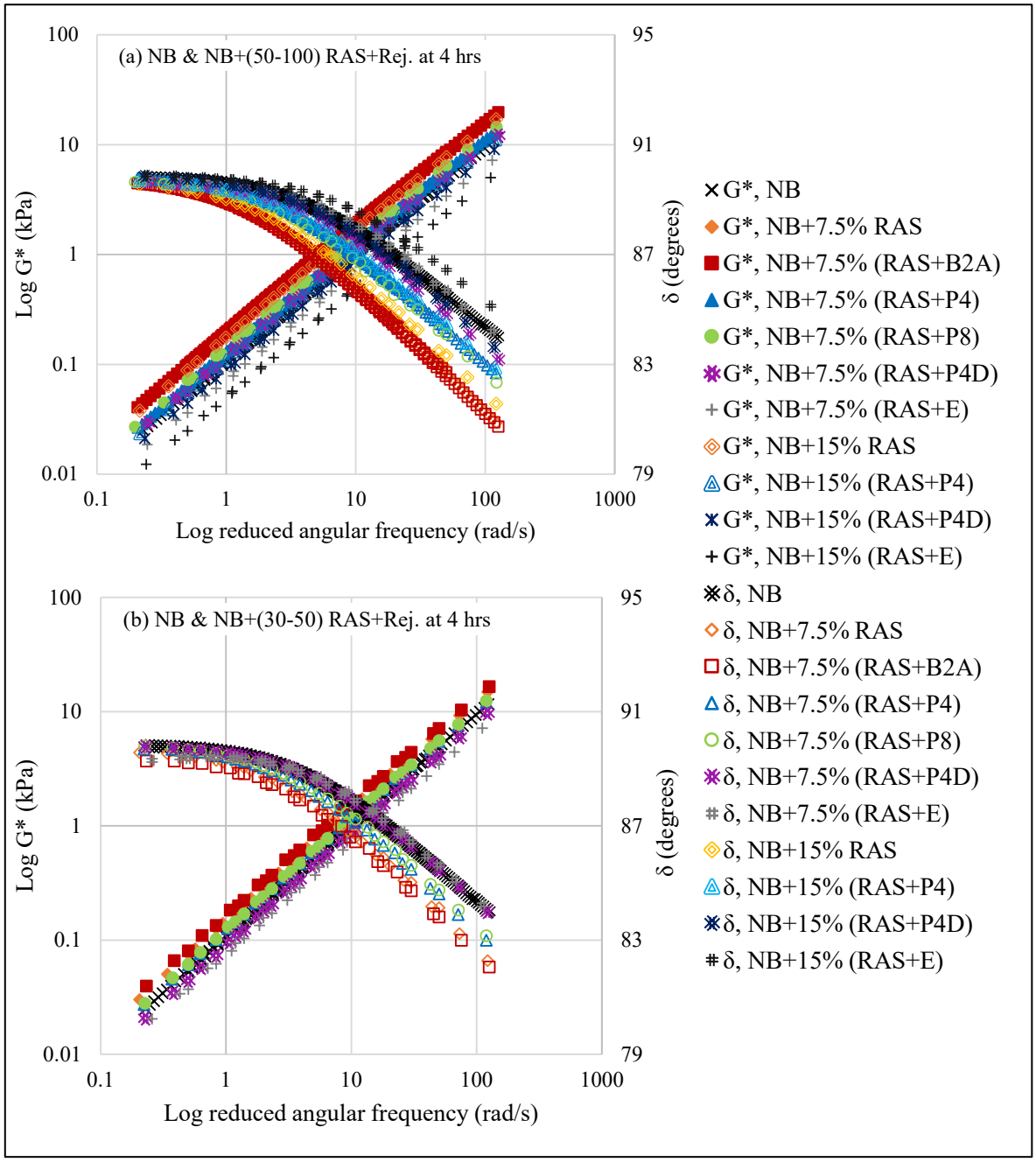

Figure 10: Master Curves for the Original Neat and Modified Binders with (a) 50-100 RAS Plus Rejuvenators and (b) 30-50 RAS Plus Rejuvenators Interacted at 4 hrs

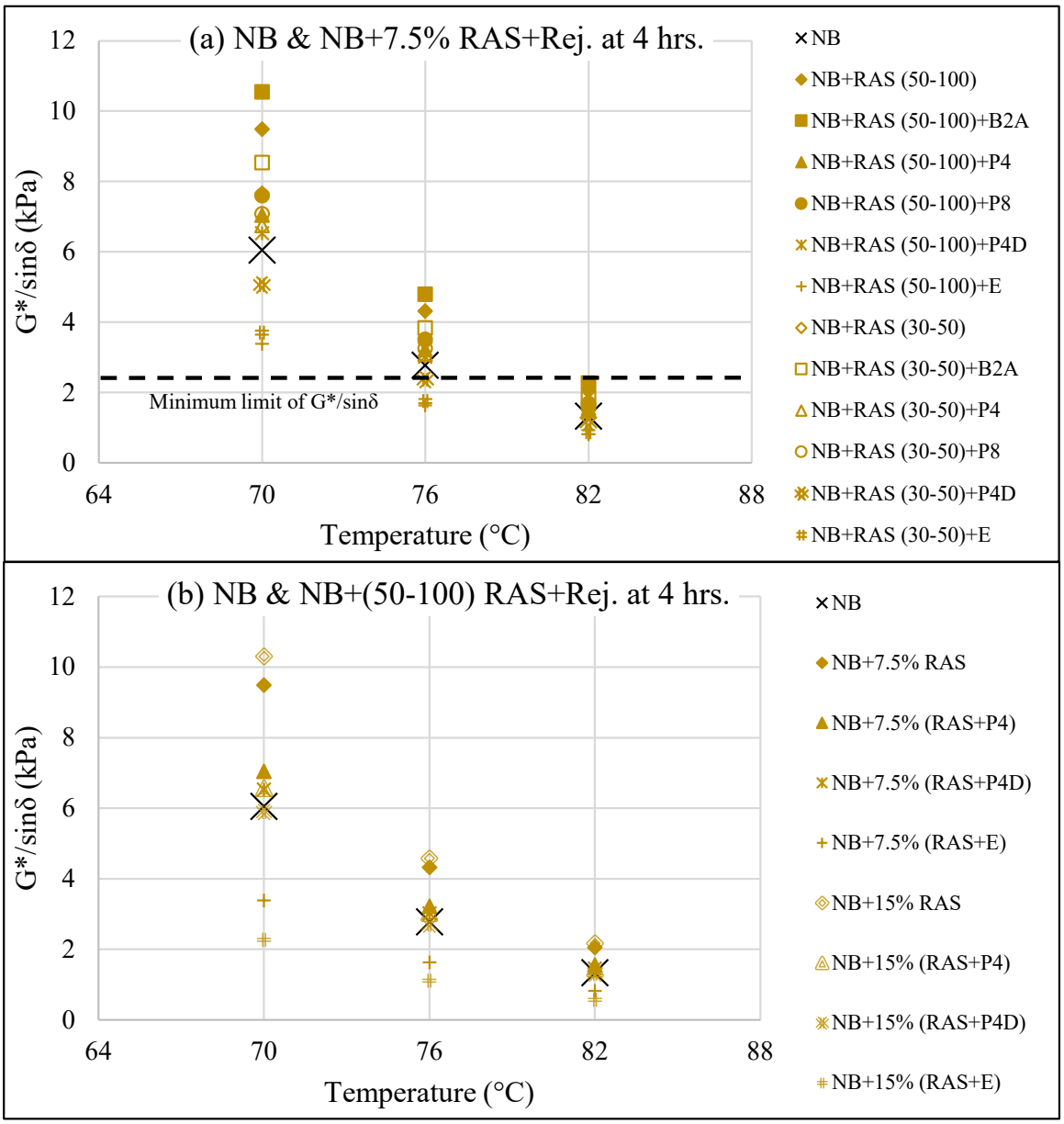

Figure 11: Temperature Sweep Results for the RTFO Neat and Modified Binders with (a) 7.5% RAS Plus Rejuvenators and (b) 50-100 RAS Plus Rejuvenators Interacted at 4 hrs

The PGs of the neat and modified asphalt binders are shown in Figure 14-a. The high PG temperatures did not change for most modified asphalt binders when compared to the value of the neat binder. However, the high PG temperatures decreased for binders that contained RAS+E or, in some samples, RAS+P4D when compared to the value of the neat binder. The low PG temperatures decreased for binders containing RAS+E by one grade when compared to the low PG temperature of the neat binder. The continuous grades (CGs) of the neat and modified asphalt binders are depicted in Figure 14-b. Using RAS or RAS+B2A increased the high CG and low CG temperatures of the modified binders when compared to the values of the neat binder. However, using RAS+E and RAS+P4D in asphalt binders showed the best enhancement in the high CG and low CG temperatures, followed by binders modified by RAS+P4 and RAS+P8.

The intermediate PG and CG temperatures for the neat and modified asphalt binders are deemed in Figure 15. Using (50-100) RAS did not significantly alter the intermediate temperatures when compared to the value of the neat binder; however, the use of (30-50) RAS in asphalt binder enhances the fatigue resistance by showing lower intermediate temperatures when compared to the neat binder's intermediate temperature. The best enhancement in the intermediate temperatures was obtained for binders modified by RAS+E and followed by RAS+P4D. These binders had the lowest intermediate PG and CG temperatures. Binders modified by (30-50) RAS had better fatigue resistance than binders modified by (50-100) RAS by presenting lower intermediate temperatures.

The relationships between the percentages of increase/decrease in high, intermediate, and low CG temperatures were evaluated and analyzed in Figure 16. These percentages were calculated for the CG temperatures of the modified asphalt binders at the 4-hrs interaction time when compared to the values of the neat binder. Direct relationships were observed between the

percentages of increase/decrease in high, intermediate, and low temperatures. Modified asphalt binders with the highest percentage decrease in high CG temperature had the highest percentage decrease in low CG temperature and the highest percentage decrease in intermediate CG temperature (e.g., NB+15% (RAS+E)). Furthermore, it can be concluded that E oil counteracted the effect of the oxidized air-blown binder included in the RAS. Asphalt binders containing RAS+E have the highest percentage decrease in high, intermediate, and low CG temperatures. Thus, Evoflex as a commercial rejuvenator is recommended to be used with asphalt binders including RAS, when compared to the efficiency of other oils used in this study (pyrolysis oils). P4 oil is considered the best type among the pyrolysis oils that frustrated the negative impact of the oxidized air-blown binder in RAS.

3.5. Insoluble Asphalt Percentage Results

The insoluble asphalt percentages were shown in Figure 17 for the original neat and modified binders that interacted at 4 hrs. The insoluble percentage for RAS (30-50) was 84.3%, and the insoluble percentage for RAS (50-100) was 83.8%. The neat binder had the lowest percentage, with a value of 0.01%. The modified asphalt binders with 7.5% RAS or 7.5% RAS that interacted with oils had insoluble percentages of less than 1.8%, and these percentages were higher than the neat binder's percentage because of the stiff binder in the RAS.

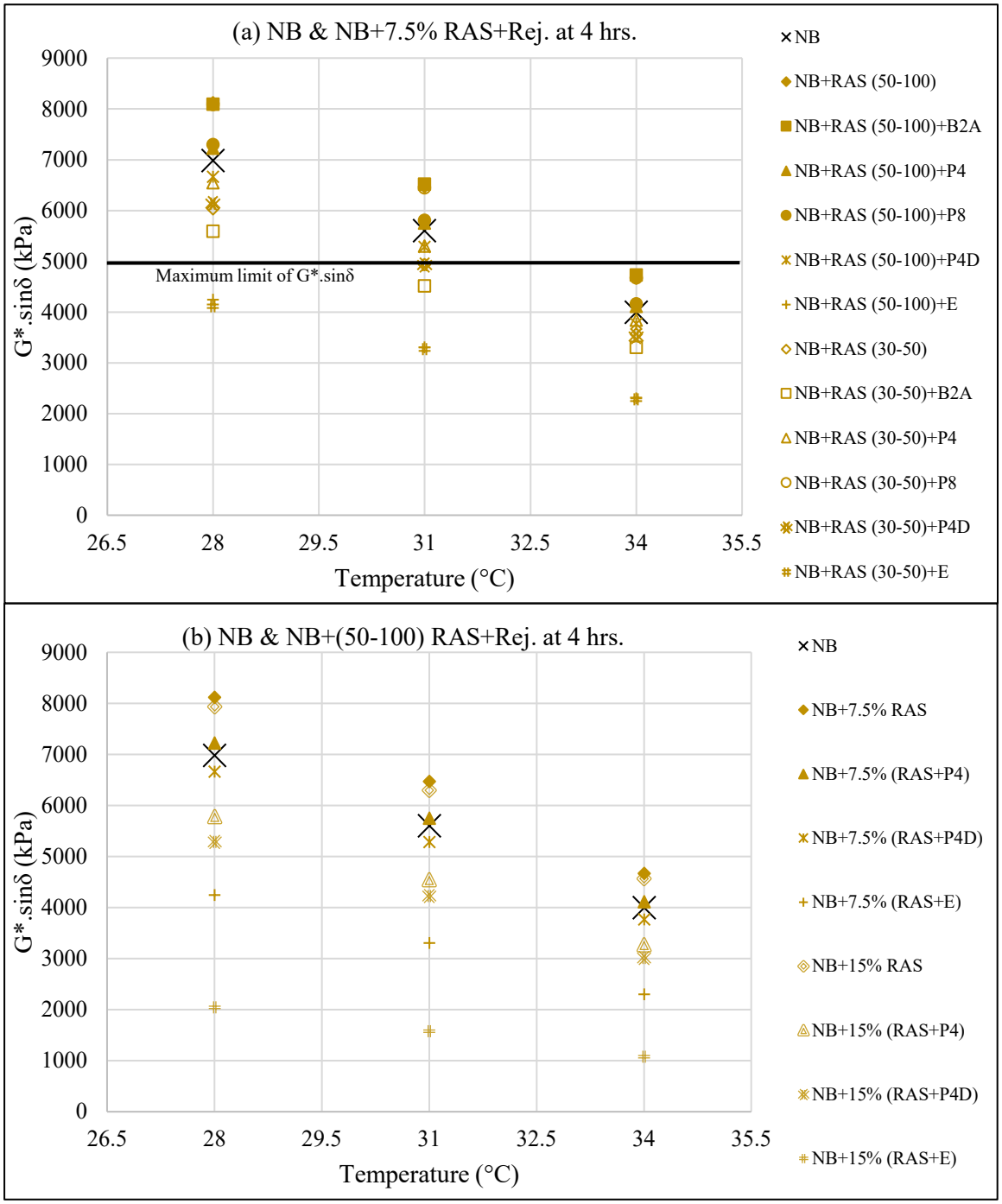

Figure 12: Temperature Sweep Results for the PAV Neat and Modified Binders with (a) 7.5% RAS Plus Rejuvenators and (b) 50-100 RAS Plus Rejuvenators Interacted at 4 hrs

Moreover, increasing the RAS or the interacted RAS with oils in the modified binders increased the insoluble asphalt percentage. No specific trend was concluded when comparing the insolubility asphalt percentages of the modified binders with a 30-50 RAS plus oils or a 50-100 RAS plus oils.

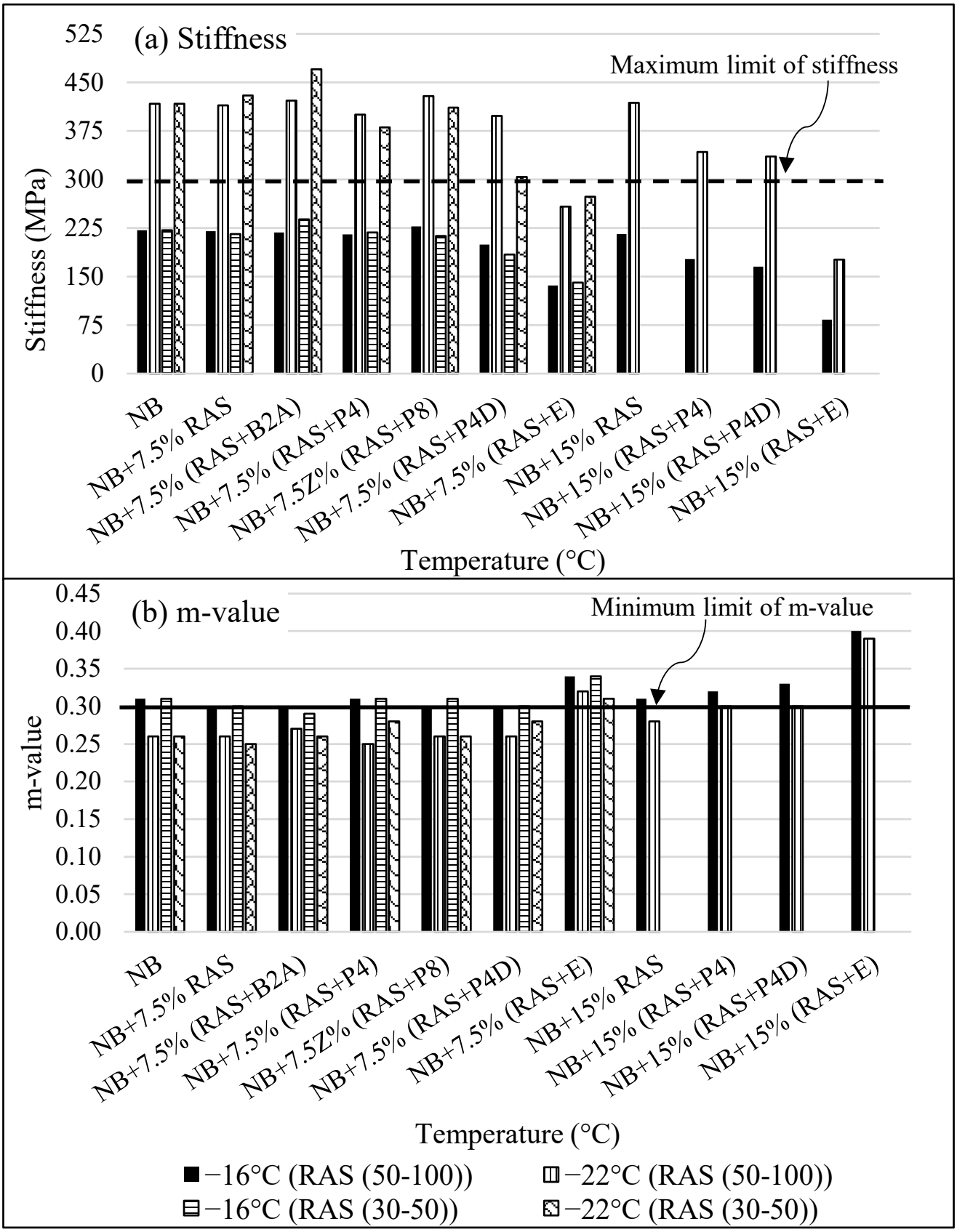

Figure 13: (a) Stiffness and (b) m-value of the PAV Neat and Modified Binders Interacted at 4 hrs

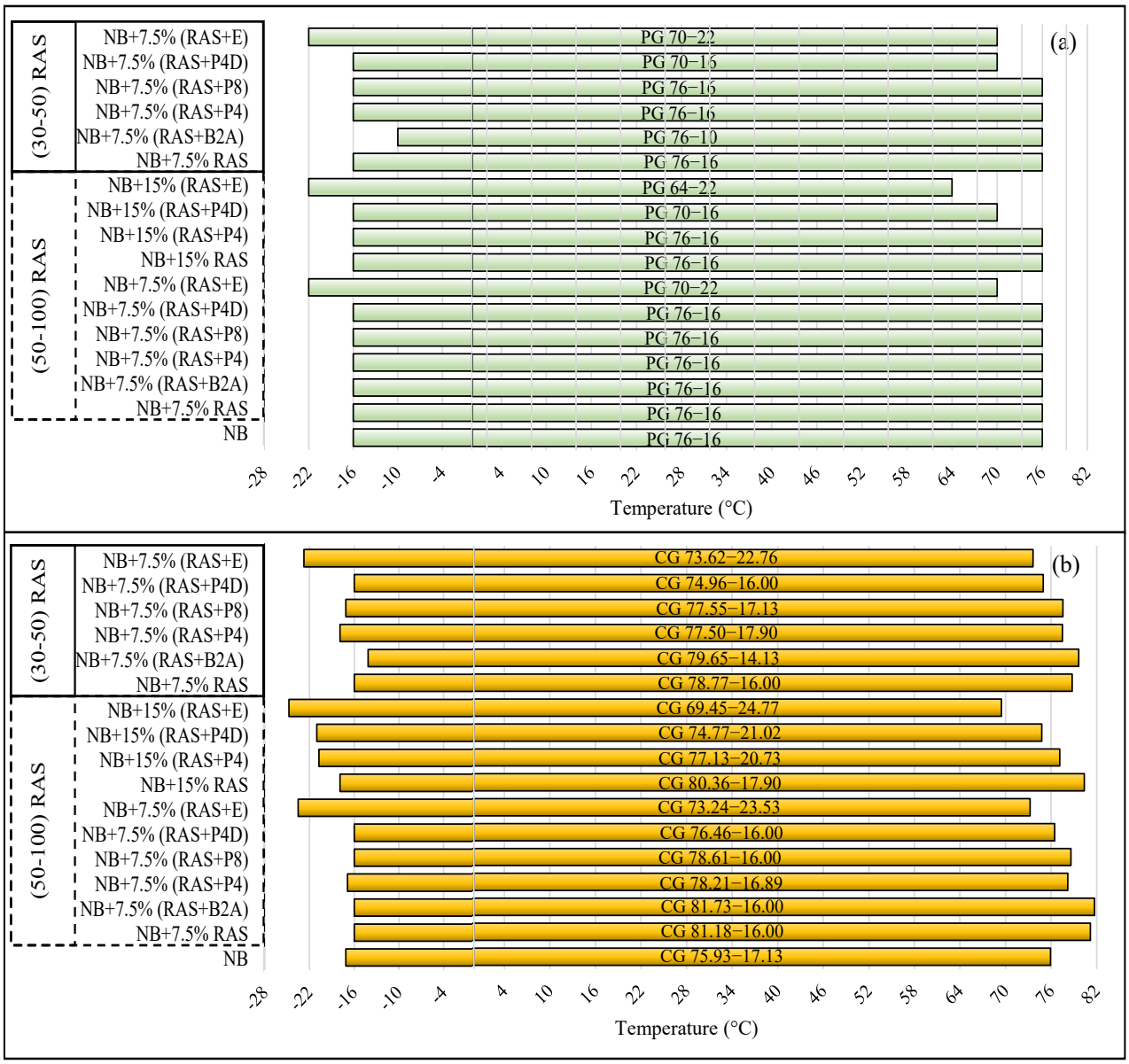

Figure 14: (a) Performance Grade and (b) Continuous Grade of Neat and Modified Asphalt Binders Interacted at 4 hrs

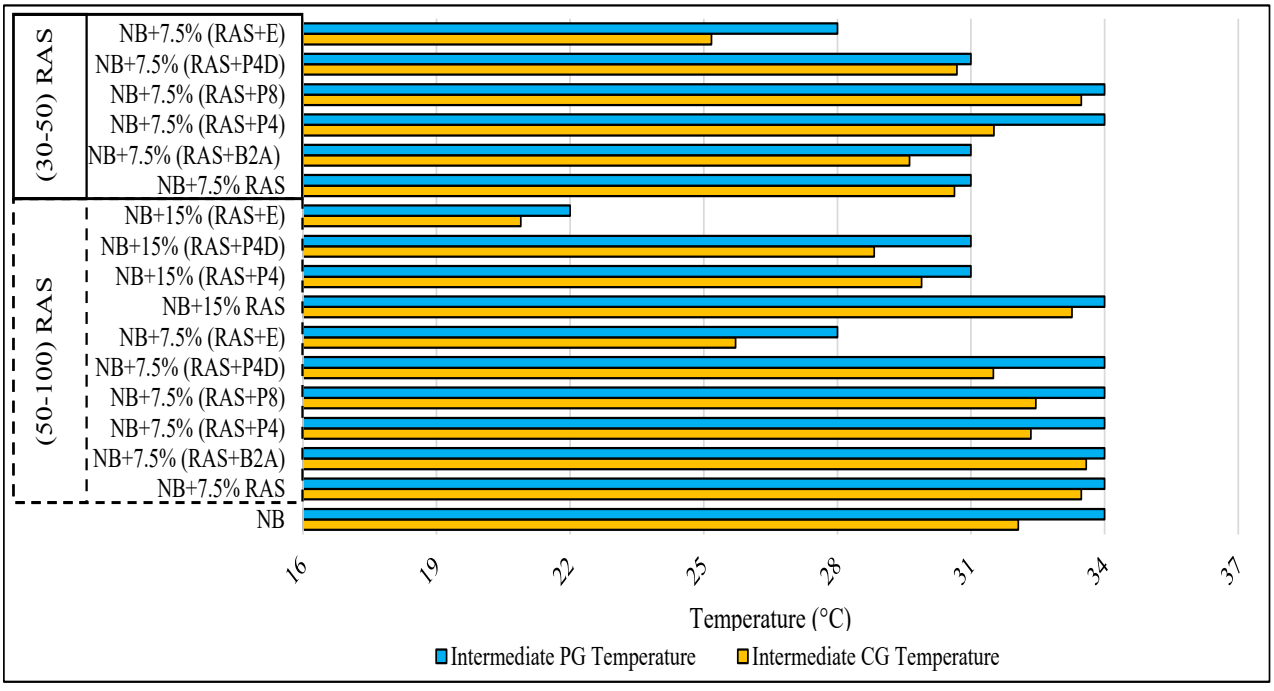

Figure 15: Intermediate PG and CG Temperatures of Neat and Modified Asphalt Binders Interacted at 4 hrs

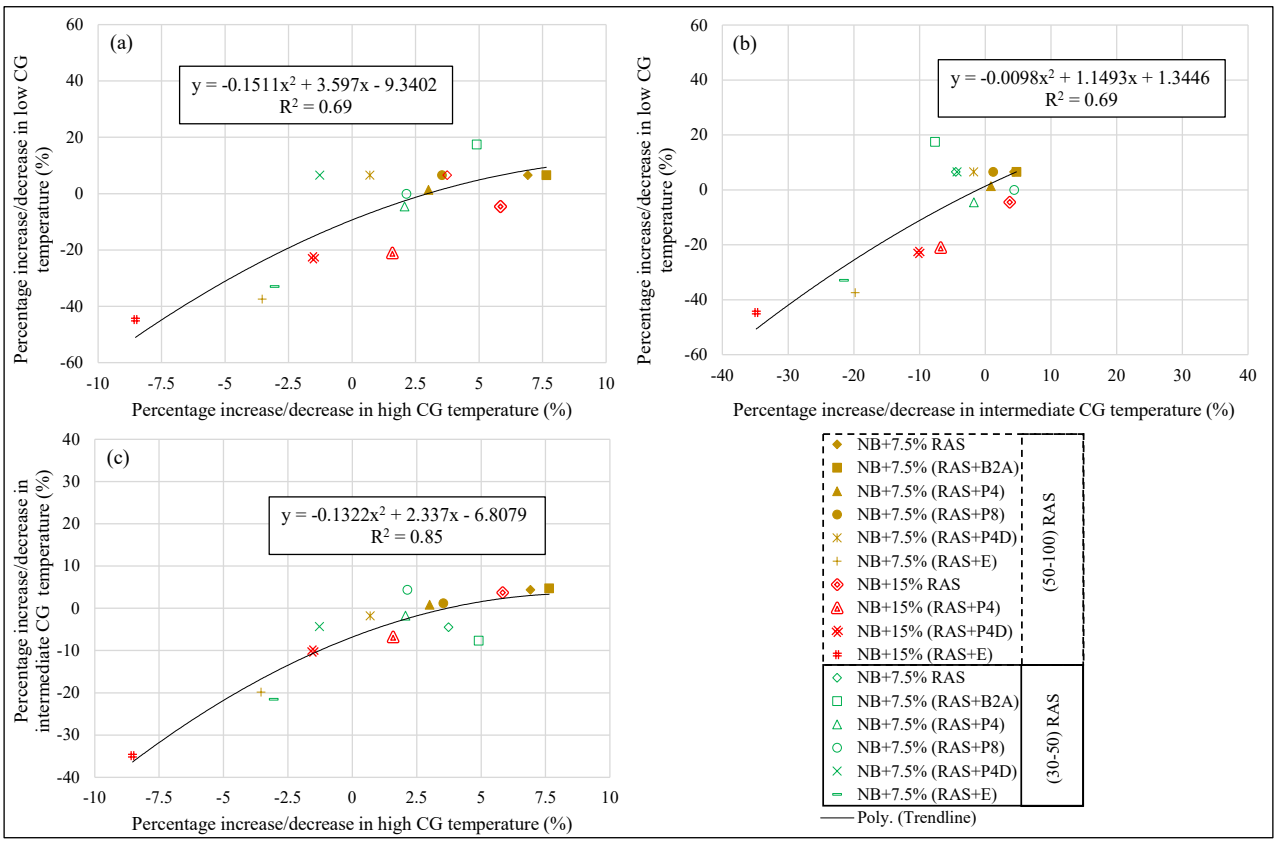

Figure 16: Relationships between the Percentages Increase/Decrease in (a) High and Low CG Temperatures, (b) Low and Intermediate CG Temperatures, and (c) High and Intermediate CG Temperatures

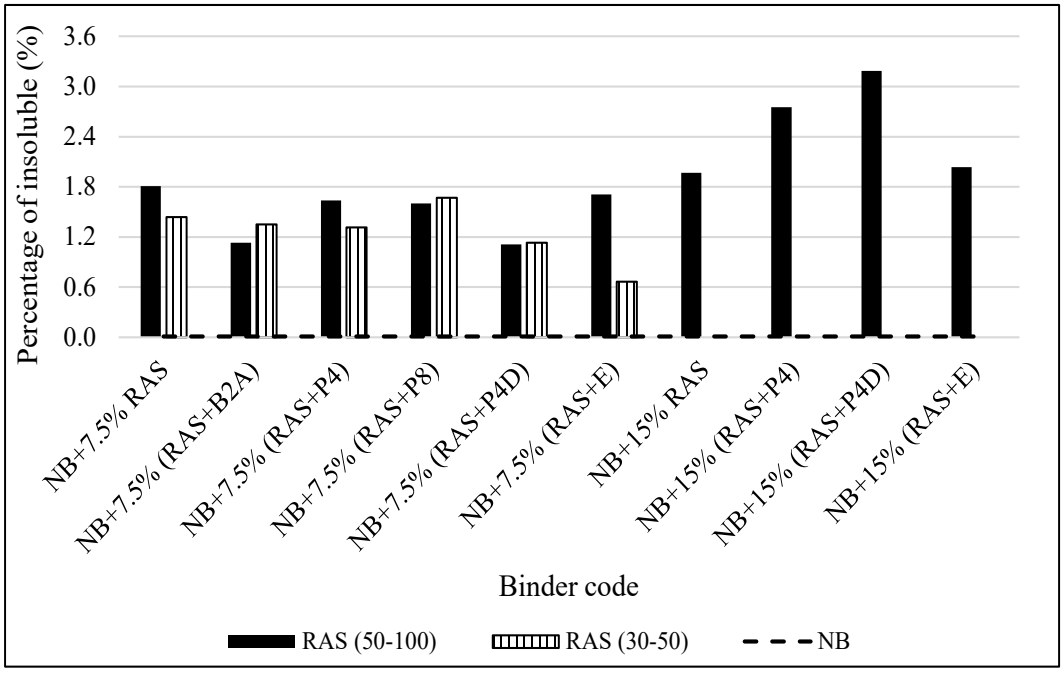

Figure 17: Insoluble Percentages of the Original Neat and Modified Binders Interacted at 4 hrs

4. Conclusions

An innovative technique was followed in this study to enhance the compatibility between RAS and asphalt binders. This was accomplished by interacting the milled RAS particles with rejuvenators to absorb low-molecular-weight fractions (aromatics) before mixing with the asphalt binder. Four pyrolysis oils and one recycling agent were used as rejuvenators. Based on this study, the following conclusions were reached:

- Interacting the milled RAS particles with rejuvenators decreases the stiffness of the oxidized air-blown binder in RAS by absorbing aromatics from rejuvenators
- Milled RAS with a particle size of 50-100 absorbed more oils, interacted more with oils, and were more compatible with the binder than RAS particles with a particle size of 30-50.

- Increasing the interaction time boosted the compatibility occurred between the RAS binder and neat binder.
- Adding Evoflex or P4D oils to RAS counteracted the impact of the oxidized air-blown binder in the RAS.
- By comparing the properties of the modified binders with RAS+B2A, RAS+P4, and RAS+P8, the modified binder with RAS+P4 was the best choice.

Conflict of Interest

The authors declare no conflict of interest.

Acknowledgment

The authors acknowledge the funding support of CarbonCycle LLC. for supporting the research and providing the pyrolysis oil samples.

Author Contributions

The authors confirm their contribution to the paper as follows: study conception and design: Abdelrahman and Deef-Allah; data collection: Deef-Allah and Abdelrahman; analysis and interpretation of results: Deef-Allah and Abdelrahman; draft manuscript preparation: Deef-Allah and Abdelrahman. All authors reviewed the results and approved the final version of the manuscript.

References

[1] J. Davis, Using Recycled Asphalt Shingles in Asphalt Pavements. Asphalt: The magazine of the asphalt institute. http://asphaltmagazine.com/using-recycled-asphalt-shingles-in-asphalt-pavements/. Accessed July. 11, 2022.

[2] J.R. Willis, P. Turner, Characterization of Asphalt Binder Extracted from Reclaimed Asphalt Shingles, Publication NCAT Report 16-01, National Center for Asphalt Technology, Auburn, AL, USA, 2016.

[3] B. Rubino, An Investigative Look at the Effects of Post Consumer Recycled Asphalt Shingles on Soils and Flexible Pavements, M.Sc. Thesis, Iowa State University, Ames, IA, USA, 2010.

[4] W.G. Buttlar, M. Abdelrahman, H. Majidifard, E. Deef-Allah, Understanding and Improving Heterogeneous, Modern Recycled Asphalt Mixes, cmr 21-007, University of Missouri, Columbia, MO, USA, 2021.

[5] E. Deef-Allah, M. Abdelrahman, M. Ragab, "Components' Exchanges between Recycled Materials and Asphalt Binders in Asphalt Mixes," *Advances. In Civil Engineering Materials*, vol. 11, no. 1, pp. 20210105, 2022, doi:10.1520/ACEM20210105.

[6] E. Deef-Allah, M. Abdelrahman, "Evaluating the Low-Temperature Properties of Asphalt Binders Extracted from Mixtures Containing Recycled Materials," Periodica Polytechnica Civil Engineering, vol. 66, no. 2, pp. 593–602, 2022, doi:10.3311/PPci.19681.

[7] G.W. Maupin, Investigation of the Use of Tear-Off Shingles in Asphalt Concrete, FHWA/VTRC 10-R23, Virginia Transportation Research Council, Charlottesville, VA, USA, 2010.

[8] E. Johnson, G. Johnson, S. Dai, D. Linell, J. McGraw, M. Watson, Incorporation of Recycled Asphalt Shingles in Hot-Mixed Asphalt Pavement Mixtures, MN/RC 2010-08, Minnesota Department of Transportation., Maplewood, MN, USA, Tech. 2010.

[9] R.C. Williams, A. Cascione, D.S. Haugen, W.G. Buttlar, R.A. Bentsen, J. Behnke, Characterization of Hot Mix Asphalt Containing Post-Consumer Recycled Asphalt Shingles and Fractionated Reclaimed Asphalt Pavement, Iowa State Univ., Ames, IA, 2011.

[10] A. Alvergue, M. Elseifi, L.N. Mohammad, S.B. Cooper, S. Cooper, "Laboratory Evaluation of Asphalt Mixtures with Reclaimed Asphalt Shingle Prepared Using the Wet Process," Road Materials and Pavement Design, vol. 15, no. sup1, pp. 62–77, 2014, doi:10.1080/14680629.2014.927410.

[11] F. Zhou, H. Li, S. Hu, J. W. Button, J.A. Epps, Characterization and Best Use of Recycled Asphalt Shingles in Hot-Mix Asphalt, FHWA/TX-13/0-6614-2, Texas A&M Transportation Institute, College Station, TX, USA, 2013.

[12] R. West, N. Tran, A. Kvasnak, B. Powell, P. Turner, "Construction and Field Performance of Hot Mix Asphalt with Moderate and High RAP Contents," in *Bearing Capacity Roads, Railways Airfields. 8th Int. Conf. (BCR2A'09)*, Champaign, IL, USA, pp. 1373–1381, 2009, doi:10.1201/9780203865286.ch143.

[13] M.Z. Alavi, D. Jones, Y. He, P. Chavez, Y. Liang, Investigation of the Effect of Reclaimed Asphalt Pavement and Reclaimed Asphalt Shingles on the Performance Properties of Asphalt Binders: Phase 1 Laboratory Testing, UCPRC-RR-2016-06, University of California Pavement Research Center, Davis, CA, USA, 2016.

[14] E. Deef-Allah, M. Abdelrahman, "Characterization of Asphalt Binders Extracted from Field Mixtures Containing RAP and/or RAS," *World Journal of Advanced Research and Reviews*, vol. 13, no. 1, pp. 140–152, 2022, doi:10.30574/wjarr.2022.13.1.0729.

[15] E. Deef-Allah, M. Abdelrahman, "Interactions between RAP and Virgin Asphalt Binders in Field, Plant, and Lab Mixes," World Journal of Advanced Research and Reviews, vol. 13, no. 1, pp. 231–249, 2022, doi:10.30574/wjarr.2022.13.1.0744.

[16] E. Deef-Allah, M. Abdelrahman, "Optimizing Percentages of Asphalt Content Extracted from Mixes Containing RAP and/or RAS," *Journal of Engineering Research and Reports*, vol. 21, no. 11, pp. 11–29, 2021, doi:10.9734/jerr/2021/v21i1117500.

[17] M. Mohammadafzali, H. Ali, J.A. Musselman, G.A. Sholar, A. Massahi, "The Effect of Aging on the Cracking Resistance of Recycled Asphalt," *Advances in Civil Engineering*, vol. 2017, pp. 1–7, 2017, doi:10.1155/2017/7240462.

[18] R. Rahbar-Rastegar, "Cracking in Asphalt Pavements: Impact of Component Properties and Aging on Fatigue and Thermal Cracking," *Ph.D. Dissertation*, University of New Hampshire, NH, USA, 2017.

[19] M.A. Elseifi, A. Alvergue, L.N. Mohammad, S. Salari, J.P. Aguiar-Moya, S.B. Cooper, "Rutting and Fatigue Behaviors of Shingle-Modified Asphalt Binders," *Journal of Materials in Civil Engineering*, vol. 28, no. 2, pp. 04015113, 2016, doi:10.1061/(ASCE)MT.1943-5533.0001400.

[20] A.R. Abbas, U.A. Mannan, S. Dessouky, "Effect of Recycled Asphalt Shingles on Physical and Chemical Properties of Virgin Asphalt Binders," *Construction and Building Materials*, vol. 45, pp. 162–172, 2013, doi:10.1016/j.conbuildmat.2013.03.073.

[21] E. Deef-Allah, M. Abdelrahman, "Investigating the Relationship between the Fatigue Cracking Resistance and Thermal Characteristics of Asphalt Binders Extracted from Field Mixes Containing Recycled Materials," *Transportation Engineering*, vol. 4, pp. 100055, 2021, doi:10.1016/j.treng.2021.100055.

[22] E. Deef-Allah, M. Abdelrahman, "Thermal, Chemical and Rheological Properties of Asphalt Binders Extracted from Field Cores," *Innovative Infrastructure Solutions*, vol. 7, no. 235, 2022, doi:10.1007/s41062-022-00836-6.

[23] H.U. Bahia, D. Swiertz, Design System for HMA Containing a High Percentage of RAS Material. University of Wisconsin-Madison

Madison, WI, USA, 2011.

[24] E. Deef-Allah, M. Abdelrahman, M. Fitch, M. Ragab, M. Bose, X. He, "Balancing the Performance and Environmental Concerns of Used Motor Oil as Rejuvenator in Asphalt Mixes," *Recycling*, vol. 4, no. 1, 2019, doi:10.3390/recycling4010011.

[25] E. Deef-Allah, M. Abdelrahman, "Effect of Used Motor Oil as a Rejuvenator on Crumb Rubber Modifier's Released Components to Asphalt Binder," *Progress in Rubber, Plastics and Recycling Technology*, vol. 37, no. 2, pp. 87–114, 2021, doi:10.1177/1477760620918600.

[26] E. Deef-Allah, M. Abdelrahman, "Balancing the Performance of Asphalt Binder Modified by Tire Rubber and Used Motor Oil," *International Journal of Recent Technology and Engineering*, vol. 8, no. 4, pp. 5501–5508, 2019, doi:10.35940/ijrte.D8893.118419.

[27] G. Guduru, C. Kumara, B. Gottumukkala, K.K. Kuna, "Effectiveness of Different Categories of Rejuvenators in Recycled Asphalt Mixtures," *Journal of Transportation Engineering, Part B: Pavements*, vol. 147, no. 2, pp. 04021006, 2021, doi:10.1061/JPEODX.0000255.

[28] G. Zhang, F. Chen, Y. Zhang, L. Zhao, J. Chen, L. Cao, J. Gao, C. Xu, "Properties and Utilization of Waste Tire Pyrolysis Oil: A Mini Review," *Fuel Processing Technology*, vol. 211, pp. 106582, 2021, doi:10.1016/j.fuproc.2020.106582.

[29] D. Czajczyńska, R. Krzyżyńska, H. Jouhara, N. Spencer, "Use of Pyrolytic Gas from Waste Tire as a Fuel: A Review," *Energy*, vol. 134, pp. 1121–1131, 2017, doi:10.1016/j.energy.2017.05.042.

[30] A. Kumar, R. Choudhary, A. Kumar, "Evaluation of Waste Tire Pyrolytic Oil as a Rejuvenation Agent for Unmodified, Polymer-Modified, and Rubber-Modified Aged Asphalt Binders," *Journal of Materials in Civil Engineering*, vol. 34, no. 10, 2022, doi:10.1061/(ASCE)MT.1943-5533.0004400.

[31] P.T. Williams, "Pyrolysis of Waste Tyres: A Review," *Waste Management*, vol. 33, no. 8, pp. 1714–1728, 2013, doi:10.1016/j.wasman.2013.05.003.

[32] ASTM D2872-19, "Standard Test Method for Effect of Heat and Air on a Moving Film of Asphalt (Rolling Thin-Film Oven Test)," West Conshohocken, PA: ASTM International, 2019, doi:10.1520/D2872-19.

[33] ASTM D6521-19a, "Standard Practice for Accelerated Aging of Asphalt Binder Using a Pressurized Aging Vessel (PAV)," West Conshohocken, PA: ASTM International, 2022, doi: 10.1520/D6521-19A.

[34] ASTM D7175-15, "Standard Test Method for Determining the Rheological Properties of Asphalt Binder Using a Dynamic Shear Rheometer," West Conshohocken, PA: ASTM International, 2015, doi:10.1520/D7175-15.

[35] ASTM D7405-20, "Standard Test Method for Multiple Stress Creep and Recovery (MSCR) of Asphalt Binder Using a Dynamic Shear Rheometer," West Conshohocken, PA: ASTM International, 2020, doi:10.1520/D7405-20.

[36] ASTM D6648-08, "Standard Test Method for Determining the Flexural Creep Stiffness of Asphalt Binder Using the Bending Beam Rheometer (BBR)," West Conshohocken, PA: ASTM International, 2016, doi: 10.1520/D6648-08.

[37] ASTM D2042-22, "Standard Test Method for Solubility of Asphalt Materials in Trichloroethylene or Toluene," West Conshohocken, PA: ASTM International, 2022, doi:10.1520/D2042-22.

Dr. Eslam Deef-Allah has done his bachelor's degree from Zagazig University in 2009. He has done his master's degree from Zagazig University in 2015. He has completed his Ph.D. degree from Missouri S&T in 2022.

Deef-Allah has more than 25 publications in peer-reviewed journal papers, peer-reviewed reports, and peer-reviewed conference proceedings. He has over 12 years of experience in research and teaching activities. The areas of experience are the characterization of modified asphalt binders with polymers or recycled materials, evaluation of the extracted and recovered asphalt binders from mixes containing recycled materials, life cycle cost analysis, and assessing alternatives of calcined bauxite to be used in the high friction surface treatment application.

Prof. Magdy Abdelrahman has done his bachelor's degree from Zagazig University in 1983. He has done his master's degree from Zagazig University in 1988. He has completed his Ph.D. degree from the University of Illinois at Urbana-Champaign in 1996.

Abdelrahman, Missouri Asphalt Pavement Association (MAPA) Endowed Professor, has published more than 100 publications in reputable international journals and conference proceedings. Research, industry, and teaching experiences are in the area of infrastructure sustainability with applications in pavement design, materials, and performance. Focus is on the interdisciplinarity aspects of infrastructure sustainability; making civil engineering more fundamental and more scientific. Integrating research into educational programs. National and international recognition. Service in national committees on construction/pavement areas. An expert in asphalt modifications including the use of recycled modifiers in civil/construction applications.